
Protein Translocon at the Outer Envelope of Chloroplasts

Aleksandar Vojta



München 2006

Protein Translocon at the Outer Envelope of Chloroplasts

Aleksandar Vojta

Dissertation
an der Fakultät für Biologie
der Ludwig–Maximilians–Universität
München

vorgelegt von
Aleksandar Vojta
aus Zagreb

München, den 06. November 2006

Erstgutachter: PD Dr. Enrico Schleiff

Zweitgutachter: Prof. Dr. Jürgen Soll

Tag der mündlichen Prüfung: 19. Dezember 2006

Contents

Abstract	viii
Zusammenfassung	ix
1 Introduction	1
1.1 The Toc complex	2
1.2 Translocation across the outer envelope	4
1.2.1 Recognition	4
1.2.2 Transfer	5
1.2.3 Translocation	7
1.3 The Tic complex	8
1.4 Proteoliposomes as a model for import	9
1.5 Aim of this work	9
2 Materials and Methods	11
2.1 Materials	11
2.1.1 Buffers, salts and other general chemicals	11
2.1.2 Detergents	11
2.1.3 Plants	11
2.1.4 Enzymes and kits	12
2.1.5 Bacterial strains, vectors and oligonucleotides	12
2.1.6 Nitrocellulose membranes	12
2.1.7 Antibodies	13
2.1.8 Column materials	13
2.1.9 Analytical reagents and accessories	13
2.1.10 Lipids	13
2.2 Methods	13
2.2.1 General procedures	13
2.2.2 Lipid and liposome methods	14
2.2.3 Analytical and visualisation methods	16
2.2.4 Biochemical methods	17
2.2.5 Gene chip analysis	19

3	Results	20
3.1	Liposomes as a tool for complex investigation	20
3.1.1	Liposome stability	20
3.1.2	Liposome size determination by dynamic light scattering and electron microscopy	22
3.1.3	Liposome solubilization	24
3.1.4	Determination of liposome size by absorption spectroscopy	25
3.1.5	Theoretical explanation	29
3.1.6	A proposed method for size determination	31
3.2	Toc complex isolation	31
3.3	Function and localization of Toc159	34
3.3.1	Expression of Toc159	34
3.3.2	Localization of Toc159	37
3.4	Translocon subunits in green and non-green tissues	40
3.4.1	Gene expression of the Toc components	40
3.4.2	Gene expression of the Tic components	44
3.4.3	Protein level of the Toc and Tic components	44
4	Discussion	46
4.1	Toc complex reconstitution	46
4.1.1	A new technique for liposome size determination	46
4.1.2	Purification and reconstitution of the Toc complex	46
4.2	Toc159 is a membrane inserted protein	47
4.3	Toc complexes with different subunit compositions	48
4.3.1	Expression in green and non-green tissues	48
4.3.2	Expression of different subunits	49
4.4	The current model of protein translocation into chloroplasts	50
5	Conclusion	53
A	Abbreviations	55
	Bibliography	56
	Acknowledgements	65

List of Figures

1.1	Stoichiometry and topology of the Toc core complex	3
1.2	The mechanism of Toc complex action	6
3.1	Stability of liposomes in different buffer conditions	21
3.2	Liposome analysis	22
3.3	Liposome size determination by DLS	23
3.4	Liposome solubilization by dodecylmaltoside and octylglucoside	24
3.5	Liposome size determination by absorption spectroscopy	26
3.6	Absorption spectra of liposomes	27
3.7	Scattering efficiency calculation	28
3.8	Calculation of liposome concentration and size	29
3.9	Optimization of Toc159 expression	36
3.10	Isolation of Toc159 out of the soluble cell extract	38
3.11	Coimmunoprecipitation	38
3.12	Liposome control	39
3.13	Gene expression of Toc components	41
3.14	Gene expression of Tic components	42
3.15	Analysis of protein amounts	44
4.1	Different Toc complexes with distinct functions	51

List of Tables

2.1	Cloning primers	14
2.2	Lipid composition of chloroplast envelopes	15
3.1	Detergent properties	32
3.2	Expression of Toc159 at different temperatures	34
3.3	Tested <i>E. coli</i> expression strains	35
3.4	Gene expression and protein ratio of the components of the plastid preprotein translocon	40
3.5	Protein ratio in chloroplasts and amyloplasts	43

Abstract

The first step of preprotein translocation across the membranes of chloroplasts is facilitated by the Toc translocon. Aim of this work was to elucidate the dynamics and the mechanism of action of this molecular machine. The central, stably associated part of the Toc translocon, the Toc core complex, consists of the pore forming Toc75 and two receptors with GTPase activity, Toc34 and Toc159.

The question of Toc159 localization was addressed since controversial results on this topic were reported. In this study, membrane localization of Toc159 was confirmed, which has further implications on the mode of its action.

To understand the necessity of multiple isoforms of Toc components as found in *Arabidopsis thaliana*, expression analysis and tissue-specific localization were conducted. Gathered data suggested the existence of several types of the complex, assembled from different types of subunits. These complexes have different preprotein specificities. Expression analysis provided further arguments for dynamic association of the intermembrane space complex with the Toc core complex. Comparison of gene expression and protein presence of translocon subunits contradicts the function of Tic20 as a general pore for stromal targeted proteins, but not as a protein conducting channel *per se*.

For further analysis of the Toc translocon structure and function, its purification and reconstitution into proteoliposomes was reinvestigated. To this end, a technique for liposome size determination in a single spectrophotometric measurement was developed.

Zusammenfassung

Der Transport von Vorstufenproteinen über äußere chloroplastidäre Hüllmembran wird durch den Toc Komplex katalysiert. Die vorgelegte Arbeit strebte nach einer Erklärung der Dynamik und Wirkungsmechanismus dieser Maschine. Der zentrale, stabil assoziierte Teil des Apparates wird Toc Kernkomplex genannt. Dieser besteht aus dem porenbildenden Toc75 und zwei Rezeptoren, Toc34 und Toc159, die GTPase Aktivität aufweisen.

Obwohl als zentrale Komponente beschrieben, wurde die Lokalisierung von Toc159 kontrovers diskutiert. Durch die im Rahmen dieser Arbeit generierten Ergebnisse konnte eindeutig nachgewiesen werden, dass Toc159 ein Membranprotein ist, was weitere Folgen für Art und Weise seiner Wirkung hat.

Um die Notwendigkeit der verschiedenen Isoformen der Translokon-Untereinheiten, wie sie in *Arabidopsis thaliana* gefunden wurden, zu verstehen, wurde eine Analyse ihrer Expression und Lokalisierung durchgeführt. Die erhaltenen Ergebnisse unterstützen die Ansicht, dass mehrere Formen des Komplexes vorhanden sind, die aus verschiedenen Isoformen gebildet werden. Solche Komplexe besitzen unterschiedliche Spezifität für Vorstufenproteine. Ausserdem hat die Expressionanalyse weitere Hinweise für eine dynamische Wechselwirkung zwischen dem Intermembranraumkomplex und dem Toc Kernkomplex erbracht. Der Vergleich der Genexpression und der Proteinmengen von Toc und Tic Untereinheiten in Chloroplasten und Hüllmembranen lässt eine Funktion von Tic20 als generelle Import Pore der inneren Membran als unwahrscheinlich erscheinen, nicht aber eine spezialisierte Funktion als proteintransportierender Kanal.

Um den Toc Kernkomplex weiter zu erforschen, war es notwendig neue Verfahren für dessen Aufreinigung und Rekonstitution in Proteoliposomen zu etablieren. Dafür wurde eine Methode entwickelt, die die Bestimmung der Größe der Liposomen in einer einzigen spektrophotometrischen Messung ermöglicht.

Chapter 1

Introduction

Chloroplasts originated in an endosymbiotic event more than 1.2 billion years ago [15], when a photosynthetic cyanobacterium was taken up by a heterotrophic cell. This event was followed by a massive transfer of genetic material to the host nucleus [67], which led to a problem for the newly established endosymbiotic relationship: proteins encoded by the transferred genes were now being synthesized in the cytosol of the host cell, and had to be transferred back to their place of action, the newly acquired organelle. Here, the chloroplast outer envelope is the first barrier for the cytosol-synthesized proteins. For a long time, the prevailing opinion was that the outer envelope of chloroplasts is like a molecular sieve—full of holes and leaky, with maybe a limited selectivity [29]. However, a significant body of recently accumulated evidence points to a tightly controlled regulation of the traffic across the outer envelope [98]. One of the gates controlling the entry of molecules into chloroplasts is the protein translocon, responsible for selection and import of protein molecules.

The first task of the complex is the recognition of chloroplastic precursor proteins which have to be imported. Most of such proteins are synthesized with a cleavable N-terminal transit sequence, which is both necessary and sufficient to target them for chloroplast import [103, 13]. Transit sequences consists of 20 to 150 amino acids, have an overall positive charge and are rich in hydroxylated amino acids [99]. The variable length and divergent primary structure suggest that it is not a specific sequence motif, but rather a certain structural characteristic, which is recognized by the receptors. For a long time it was believed that only outer envelope proteins lack an N-terminal transit sequence and some authors suggest that they might have an internal signal instead [13, 89]. However, recent proteomic approaches identified many plastid proteins without an obvious cleavable signal with the above outlined characteristics within the coding region [53]. Therefore, the characteristics of the targeting signal and translocation events will be

revisited for these proteins in future. The first hint for an alternative route in *Arabidopsis thaliana* came from the observed endoplasmic reticulum intermediate of β -carbonic anhydrase before its translocation into plastids [111].

1.1 The Toc complex

The Toc core complex consists of three types of subunits: the channel protein Toc75, two GTPases with receptor function, Toc34 and Toc159, and two less abundant Toc components, Toc64 and Toc12, which are dynamically associated with the core complex (Figure 1.1). The latter two proteins are components of an intermembrane space complex, together with isHsp70 and Tic22 [8]. Toc12 is an outer envelope protein which has a C-terminal J-domain protruding into the intermembrane space. The J-domain recruits the intermembrane space chaperone isHsp70 and stimulates its ATPase activity [8]. Toc12 also interacts with the intermembrane space part of Toc64, another member of the IMS complex, which is less well characterized than Toc core complex components. Toc64 contains three cytosolic exposed tetratricopeptide (TPR) repeats, which form a clamp-type domain [118]. This domain recognizes Hsp90 delivered precursor proteins via interaction with the Hsp90 chaperone [81]. The Tic22 protein, a member of the translocon in the intermembrane space, is thought to mediate interaction between the Toc and the Tic complex [57, 8].

Both Toc34 and Toc159 have a C-terminal transmembrane domain, and a more N-terminally located GTPase domain, which is a region of high similarity between the two receptor proteins. Unlike the smaller Toc34, the Toc159 has an additional domain at its N-terminus, the acidic A-domain. This part of the protein seems not to be essential for its function in protein translocation *in vitro*, although its presence increases yield in import experiments [17]. Hence, the role of the A-domain is still unknown.

Earlier studies [37] suggested that Toc159 might be a soluble receptor, because it was found in the cytosol as well as in the outer envelope after cell fractionation. At this point it was speculated that the soluble receptor could transfer the guidance complex to the chloroplast surface. This speculation has implications reaching further than just the mode of action of Toc159, since it suggests that Toc159, and not Toc34, acts as the primary precursor protein receptor.

The Toc core complex isolated from pea (*Pisum sativum*) has an apparent molecular mass of 500 kDa and molecular stoichiometry of 1:4:4-5 between Toc159, Toc75 and Toc34 [90]. Electron microscopic single particle analysis of isolated Toc complex revealed a toroid-shaped particle measuring 13 nm in diameter, with a protruding finger-like domain in the center, giving

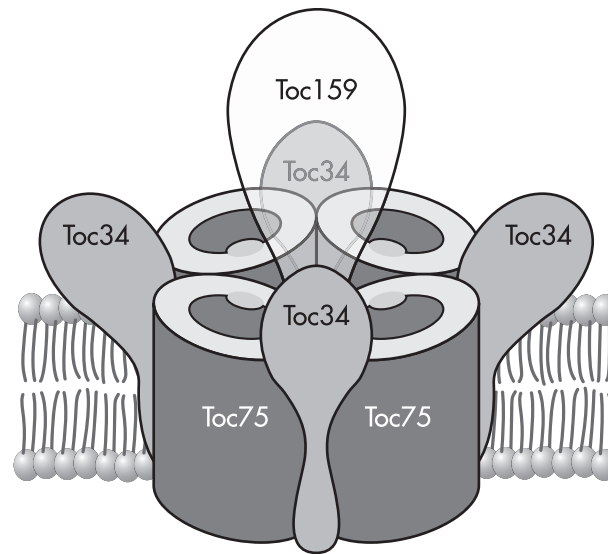


Figure 1.1: Stoichiometry and topology of the Toc core complex. The Toc core complex consists of four Toc75 and Toc34 subunits, with an additional Toc159 in the center. According to our current understanding, Toc75 proteins form four separate pores, and a single Toc159 serves all of them. The presented structure was inferred from stoichiometry data and EM images [90].

it a height of 10-12 nm, and dividing the central cavity into four apparent pores.

A second layer of complexity of the translocon was discovered when sequencing of the *Arabidopsis thaliana* genome was completed in the year 2000, as several isoforms were found for each component [72]. There are two Toc34 homologues in *A. thaliana*, namely atToc33 and atToc34. The atToc33 is regulated by phosphorylation, similar to the Toc34 from pea, while atToc34 seems to lack such regulation [45]. GTPase activity of both proteins is stimulated by precursor proteins. Different subclasses of precursor proteins bind preferentially to one or the other Toc34 isoform [9]. This specialization is not absolute, since a degree of functional overlap has been demonstrated—knockouts of atToc33 with a working copy of atToc34 are viable, although they show a relatively mild phenotype [44]. The family of Toc159 proteins in *A. thaliana* consists of atToc159, atToc132, atToc120 and atToc90 [61]. The atToc159 isoform is highly expressed in photosynthetic tissues, especially during early development, while atToc132 and atToc120 are uniformly expressed, which makes them comparably abundant in nonphotosynthetic tissues [61]. No single knockout mutant has a particularly strong phenotype, and the atToc132/atToc120 double mutant resembles the atToc159 knockout. The pore-forming Toc75 comes in two main varieties in *A. thaliana*: the most abundant outer envelope protein atToc75-III, highly expressed in growing photosynthetic tissues, and the atToc75-IV, which is uniformly expressed at a low level

[5]. Knockout of atToc75-III is embryo lethal [5]. Additionally, a pseudogene named atToc75-I belongs to the Toc75 group, due to its homology with other members. Another Toc75-like channel of the chloroplast outer envelope is the 66 kDa Toc75-V [26, 43]. It is phylogenetically more closely related to prokaryotic Toc75 ancestors than to other plant Toc75 proteins.

1.2 Translocation across the outer envelope

1.2.1 Recognition

Nascent precursor proteins are prevented from inappropriate interactions with proteins abundant in the cytosol by molecular chaperones from the Hsp70 family. They keep the polypeptide in a soluble, partly unfolded, import competent state. For some proteins with N-terminal transit peptide, early transport events are also assisted by 14-3-3 family proteins which, together with Hsp70s, form a guidance complex [68, 31] upon phosphorylation of the transit sequence [114]. This assembly is subsequently targeted to the Toc34 receptor on the chloroplast surface (Figure 1.2). However, whether this transport route is as general as discussed [99] remains under debate, as direct evidence of phosphorylation and 14-3-3 association was presented for only a small number of precursor proteins. Alternatively, a class of non-phosphorylated precursor proteins has been found to assemble with Hsp70 and Hsp90, but not with 14-3-3. These nascent precursor proteins are targeted to the cytosol exposed TPR domain of Toc64 via its interaction with the Hsp90 chaperone [81] (Figure 1.2).

The cytosolic exposed tetratricopeptide domain of Toc64 recognizes the C-terminus of Hsp90 [81] in a clamp-type manner. At this stage, Toc64 does not interact with the delivered precursor protein itself but with the Hsp90 chaperone. The recognition of the Hsp90 by Toc64 is followed by a transient interaction of Toc64 with the GTP-charged G domain of Toc34. Hence, the transfer of a precursor protein to Toc34 takes place in a GTP-dependent manner, even though the molecular mechanism is not yet explained in detail. However, Toc34^{GTP} now recognizes the transit peptide of the Hsp90 delivered precursor protein directly. At this point the 14-3-3 and the Hsp90 dependent routes for precursor protein delivery converge (Figure 1.2) as Toc34 was found to be the primary receptor of the 14-3-3 delivered precursor proteins as well [81]. Furthermore, most of the components and mechanistic steps of the way from the ribosome to the chloroplast remain to be explored in the future.

1.2.2 Transfer

The Toc34 receptor is the entry point for each precursor protein into the Toc core complex. Toc34 has to be charged with GTP in order to recognize the precursor protein [103, 46, 45]. In case of the model substrate, which is the small subunit of RuBisCO, Toc34^{GTP} recognizes the C-terminus of the transit sequence with high affinity [91]. Experimentally confirmed structure predictions suggest helical conformation of this region [13]. At the same time the N-terminal portion of the transit sequence engages with the Toc159 receptor in a nucleotide dependent manner, but only when the transit sequence is dephosphorylated [8, 96]. Details of the dephosphorylation are still unknown. The interaction of the C-terminal part of the transit sequence with Toc34 induces the subsequent hydrolysis of GTP [46]. Since the GDP loaded form of the receptor Toc34 has a low affinity for precursor proteins, this hydrolysis is paralleled by a precursor protein release from its binding pocket [45] (Figure 1.2). The released segment of the transit sequence will now be recognized by the GTP charged receptor Toc159 [8]. Thereby, the recognition of the C-terminal portion induces the GTP hydrolysis of Toc159 as well.

Recognition of the precursor protein and its processing is modulated by phosphorylation. Both GTPases are dominant phosphoproteins phosphorylated by two different kinases [30]. For Toc34 it was demonstrated that both GTP binding and precursor protein recognition is impaired after phosphorylation [103, 46, 45]. Interestingly, in *A. thaliana* only Toc33, but not Toc34, can be phosphorylated, suggesting different regulatory mechanisms for the different translocons formed. One open question is the regulation of the GTPase cycle for the two G proteins in the Toc complex. Crystal structure of Toc34 revealed that its molecules exist as dimers [101]. More recent studies indicate the possibility that Toc34 forms heterodimers with Toc159, the interaction taking place via their homologous GTP-binding domains [50]. Such an interaction could provide means for mutual activation of the two receptors thereby facilitating the precursor protein handover, and could also have a role in the assembly of the Toc core complex. However, final evidence for this notion is still missing.

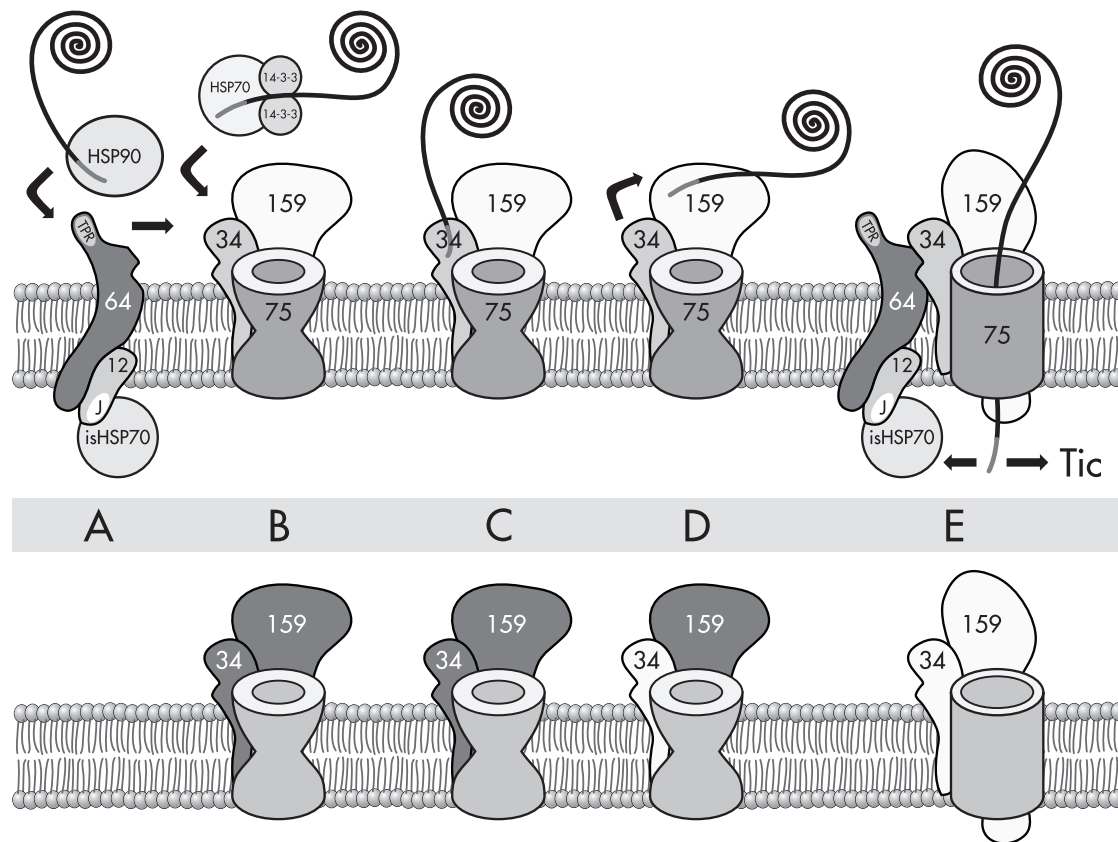


Figure 1.2: The mechanism of Toc complex action. The top portion shows a scheme of precursor protein translocation by the Toc complex. The bottom portion indicates the nucleotide state of the receptors Toc34 and Toc159 at the corresponding translocation steps. Here the GTP state is indicated by dark grey and the GDP by light grey. Additionally, the open and closed state of the pore Toc75 is indicated. (A) A precursor protein (curled thick line) containing a transit sequence (grey extension of the line) is delivered to Toc64 by a Hsp90 chaperone molecule. The TPR domain of Toc64 facilitates its interaction with Hsp90. After binding, Toc64 undergoes a transient interaction with a GTP loaded Toc34 molecule, which receives the precursor protein. (B) A second class of precursor proteins is delivered to the chloroplast surface by a so called guidance complex consisting of one Hsp70 molecule and a 14-3-3 dimer. These precursor proteins are recognised directly by Toc34. (C) After binding the transit sequence (dark gray) of a precursor protein, Toc34 hydrolyzes its bound GTP and (D) transfers the precursor protein to Toc159. Hydrolysis of GTP causes a conformational change in Toc159 (E) and the precursor protein is pushed through the translocation pore. The precursor protein is now taken over by the Tic translocon on the inner envelope. Alternatively, precursor protein could be taken over and pulled by isHsp70, delivered by Toc64/Toc12 during the interaction of Toc64 and Toc34. Toc12 contains a J domain which facilitates its interaction with chaperones in the intermembrane space (e.g. isHsp70).

1.2.3 Translocation

There is experimental evidence that precursor protein transfer across the outer envelope of chloroplast is indeed powered by the GTPase action of Toc159, which hydrolyses GTP and operates in a way that could be visualized as being similar to the operation of a sewing machine [88]. Toc159 seems to provide the only driving force for the first translocation step. An initial pulling force of chaperones can be ruled out in this phase of translocation since a minimal reconstituted system consisting of Toc159 and Toc75 is able to carry out the import reaction using GTP only [88]. However, the intermembrane space localized Hsp70 (isHsp70, [66, 113, 93]) might take over *in vivo* once the precursor protein reaches the intermembrane space after the initial transfer event catalyzed by Toc159.

The essential role of Toc159 in chloroplast biogenesis [6], and its presence in a “catalytic ratio” in the complex (1:4 to Toc75 and Toc34, [90]) support the notion of Toc159 action as a translocation motor. Here, a loose parallel with the ATPase driven SecA-type protein translocation [65] can be drawn. In both systems, the receptor itself charges the initial translocation.

But what happens after the initial stroke? Toc75 itself contains a precursor binding site [40, 28]. This might be the first recognition site in the intermembrane space. Furthermore, Toc64 interacts with the rest of the IMS complex—and directly with the Toc12. Transfer of the precursor protein to the Toc34 induces Toc64 to activate its interaction partner Toc12, which in turn recruits the ATP-loaded isHsp70 [9]. The chaperone is ready to be transferred to the precursor protein when it emerges from the translocation pore. Upon precursor protein binding, isHsp70 catalyzes the hydrolysis of its bound ATP, which is stimulated by the action of the J-domain of Toc12. This is followed by the exchange of the bound ADP for a new molecule of ATP and subsequent precursor protein release. It is generally believed that precursor proteins are immediately taken over by the Tic translocon of the inner envelope [2, 71].

For the complete picture of a feasible mechanistic model of translocation, the question of energetics has to be addressed. What drives the bulk of translocation? For mitochondrial precursor proteins recognition and transfer at the organelle surface a so-called ‘acid chain’ hypothesis was formulated [55]. It is suggested that a series of acidic receptor sites interacting with the positively charged targeting signals are strategically placed along the import pathway and drive the first steps of protein import [86]. In this model the order of binding is thought to be assured by the topological arrangement of these sites [86] and a massive short-circuiting of the pathway is probably prevented by cytosolic chaperones associated with the precursor protein. It is appealing to speculate that such a model could explain certain aspects of the chloroplast translocation. Here, on the cytosolic face of the outer envelope of chloroplasts an affinity chain is built by dif-

ferent charged G domains, whereas initial recognition is partly facilitated by an interaction with the protein involved in delivery [81]. The final intermembrane space localized binding site of this affinity chain might be within Toc75 itself [28] or might be presented by the intermembrane space localized domain of Toc64 [81]. A precursor protein already transferred into the intermembrane space might be guided further in a similar manner through the Tic complex, which lacks a protein with a motor activity or a proton gradient across the membrane in which it is embedded [99]. However, binding spots which would constitute an 'affinity chain' through the Tic complex still need to be identified.

1.3 The Tic complex

The translocon of the inner envelope can be divided into acting and regulating subunits. Tic110 [105, 35] and Tic20 [57] were suggested to participate in pore formation. Tic110 forms a cation selective channel with calculated pore opening of 1.7 nm [35]. Tic20 was shown to be essential for protein import across the inner envelope [18] and seems to be related to the Tim17/23 import channel in mitochondria [104]. Tic21, another essential component similar to Tic20, has been identified recently [104].

Regulatory subunits Tic62, Tic55 and Tic32 are components of a redox chain which regulates the translocation efficiency by sensing the redox state in the stroma [62]. The C-terminus of Tic62 faces the stroma where it interacts with ferredoxin-NAD(P)⁺ oxydoreductase, which could enable it to sense the redox state of the organelle [62]. Tic55 contains a Rieske-type iron-sulphur cluster [16] which probably acts as a redox sensor and influences the import process by its association with Tic110 [100]. Tic32 seems to exert its regulatory function by influencing the complex stability [41]. Regulation of the Tic translocon by calmoduline has been discussed, since calmoduline-specific inhibitors had influenced the translocation of pSSU [20]. Recent studies indicate that redox modulation and calcium regulation of chloroplast protein import might convene at the Tic translocon and both could be mediated by Tic32 [19]. However, the molecular mechanism of action remains largely unexplained in case of both calmoduline and redox regulation.

The function of Tic40 is still not fully explained. It has a degree of homology to heat-shock-associated proteins [21] and according to tertiary structure prediction and immunological studies contains a TPR-domain [21]. It has been suggested that it has a secondary role in protein import [59]. Tic22 is only peripherally associated with the Tic complex and is probably more important as a member of the IMS complex [58].

Upon the initial translocation through the Tic110 pore, stromal chaperones energize the sub-

sequent import steps in a similar manner as for mitochondria [86].

1.4 Proteoliposomes as a model for import

Reconstitution into synthetic liposomes is one of the major tools to investigate the function of membrane proteins, and various reconstitution protocols have been established in the past [77, 54, 80, 88]. However, it became obvious that the liposome behavior and architecture depends on the lipid composition. For example, the influence of salt on the liposome structure was found to be lipid dependent [117, 75, 38]. In addition, non-bilayer lipids can influence the liposome shape during reconstitution or subsequent experiments [76, 39]. To avoid such influences, experiments are generally performed using model lipids like phosphatidylcholine. However, there is experimental evidence that the activity of proteins in the bilayer [107, 11, 24] and the dynamic complex assembly [36] are altered by the lipid content. Furthermore, lipids characteristic for chloroplasts, such as MGDG and DGDG, occur in all photosynthetic eukaryotes. Studies based on mutants unable to synthesize such lipids suggest that they may be essential for chloroplast function, possibly due to their ability to adjust the curvature of a protein-rich membrane by action of their specifically sized headgroups [12, 90, 48]. Therefore, it will be essential to construct reconstitution systems with authentic lipid content.

A reconstituted system was recently used to study the function of the Toc complex [88, 9]. Lipid composition of the outer envelope membrane of spinach (*Spinacea oleracea*) was used to create liposomes [12]. For a better understanding of the translocation pathway, it is further necessary to reconstitute other homologues of the translocation components [99].

1.5 Aim of this work

Reconstitution into liposomes is a promising method for Toc complex investigation. To this end, obtaining the active complex in significant amounts from plant material was attempted. As a tool for protein reconstitution, a protocol that allows fast and easy estimation of liposome size and concentration in a single absorption spectroscopy measurement had to be established.

The issue of Toc159 localization was addressed, since identification of the soluble form [37] reopened the question of the initial contact of the preprotein and the core complex. Solving this question is an essential point for the understanding of the translocation mechanism.

Understanding of the function of the different isoforms of Toc components represents another essential question. Some Toc subunit isoforms were only predicted by *in silico* analysis and little

is known about their expression and stoichiometry in plants. Therefore, gene expression as well as protein levels in the envelope membrane had to be analysed to gain insight into possible functions of these proteins as well as the structure and subunit composition of the Toc complex.

Chapter 2

Materials and Methods

2.1 Materials

2.1.1 Buffers, salts and other general chemicals

All general chemicals, such as buffers, salts, sucrose, sorbitol, inorganic acids, organic solvents etc. were purchased from Sigma-Aldrich (München, Germany), Roth (Karlsruhe, Germany), Roche (Penzberg, Germany) and Merck (Darmstadt, Germany). Nucleotides were obtained from Roche Molecular Biochemicals (Mannheim, Germany).

2.1.2 Detergents

N-decyl- β -D-maltoside was supplied by Glycon GmbH (Luckenwalde, Germany); n-dodecyl- β -D-maltoside was obtained from Biomol (Hamburg, Germany). Octyl- β -D-glucoside was purchased from Roche Molecular Biochemicals (Mannheim, Germany), and Tween20 from AppliChem (Darmstadt, Germany).

2.1.3 Plants

Pea (*Pisum sativum*) seeds of the sort “Arvica” (Praha, Czech Republic) were grown on soil under light/dark cycle (12 h of light) in a climate chamber at 20°C. These plants were used for chloroplast envelope isolation. Seedlings of *Arabidopsis thaliana*, Columbia ecotype, were grown on MS plates [69] supplemented with 1% (w/v) sucrose. After 7–10 days plants were transferred on soil. The plants were grown in a climate chamber at 20°C with a 14 h/10 h light/dark cycle

at a photon flux density of $100 \mu\text{mol photons m}^{-2}\text{s}^{-1}$. Seeds were sterilized by 50% NaClO and vernalized at 4°C over night prior to transfer on MS plates.

2.1.4 Enzymes and kits

Enzymes for cloning, restriction endonucleases, T4-DNA-ligases and Taq-polymerases were obtained from Roche (Penzberg, Germany), MBI Fermentas (St. Leon-Rot, Germany) and Qiagen (Hilden, Germany). Lipase VII (from *Candida rugosa*) was purchased from Sigma Aldrich (München, Germany), RNase from Amersham Biosciences (Freiburg, Germany) and lysozyme from Serva (Heidelberg, Germany). *In vitro* protein synthesis was carried out using the RTS 100 Rapid Translation System for cell-free protein expression (Roche Diagnostics GmbH, Mannheim, Germany). DNA was purified using Plasmid Midi Kit from Macherey and Nagel (Düren, Germany) when larger quantities were required, whereas for smaller scale DNA purification the Silica Spin Kit from Biometra (Göttingen, Germany) was utilised. For isolation of RNA, RNeasy kit from Qiagen (Hilden, Germany) was used. The above listed kits were utilized according to manufacturer's instructions.

2.1.5 Bacterial strains, vectors and oligonucleotides

DH5 α *Escherichia coli* strain (GibcoBRL, Eggenstein) was used For DNA amplification. Expression of genes cloned into plasmid vectors was carried out in protease deficient BL21(DE3) cells (Novagen, Madison, USA), or when noted in BL21 Origami™ (Novagen), BL21 Star™ (Invitrogen, Carlsbad, USA) or Top10F' (Invitrogen) cells; BL21 RIL and RP competent cells were from Stratagene (La Jolla, USA). The pMICO helper plasmid used for expression of toxic proteins in *E. coli* was kindly provided by Dr. Ian Menz; more details can be found in [22]. The pRosetta helper plasmid was from Novagen (Madison, USA).

Constructs for expression were cloned in pET21d, pET24d (Novagen, Madison, USA) or pProEX HTa (Invitrogen, Carlsbad, USA) vector. Vectors for the RTS 100 expression system (pIVEX) were from Roche Diagnostics (Mannheim, Germany).

The oligonucleotides used as PCR primers were purchased from MWG Biotech AG (Ebersberg, Germany).

2.1.6 Nitrocellulose membranes

Nitrocellulose membranes (Protran BA-S83, $0.2 \mu\text{m}$) were purchased from Schleicher and Schüll (Dassel, Germany).

2.1.7 Antibodies

Primary antibodies were produced by injection of recombinantly expressed proteins into rabbits. The used antisera were raised as described [90]. Secondary antibody was affinity purified anti-rabbit IgG (whole molecule) from goat, conjugated with alkaline phosphatase, purchased from Sigma-Aldrich (München, Germany).

2.1.8 Column materials

Ni-NTA column material was supplied by Qiagen (Hilden, Germany), Protein-A Sepharose was supplied by Amersham Biosciences (Freiburg, Germany).

2.1.9 Analytical reagents and accessories

Protein concentrations were determined using Bio-Rad Laboratories protein assay (Hercules, USA). Silica gel 60 chromatography plates (10 × 10 cm) were obtained from Merck (Darmstadt, Germany).

2.1.10 Lipids

Purified plant lipids were purchased from Nutfield Nurseries (Surrey, UK). The lipids were selected to reflect the lipid composition of spinach chloroplast envelopes according to Bruce [12]: monogalactosyldiacylglyceride (MGDG), digalactosyldiacylglyceride (DGDG), sulfolipid (SL), phosphatidylcholine (PC), phosphatidylglycerol (PG) and phosphatidylinositol (PI).

2.2 Methods

2.2.1 General procedures

Proteins were separated in polyacrylamide gels essentially as described in [63]. Cloning and expression of the proteins used is described elsewhere ([97, 88, 62, 102, 46] and references therein). Chloroplasts and chloroplast envelopes were prepared from pea (*Pisum sativum*) as described [90]. Chlorophyll content of chloroplasts was determined as described in [4]. Numerical data were processed and presented using Sigma Plot (Systat Software, Point Richmond, USA). Quantitation of 2D images was performed using AIDA software (Raytest, Straubenhardt, Germany) or ScionImage (Scion Corporation, Frederick, USA).

Cloning, expression and purification of Toc159

The *atToc159* full length gene was cloned in an expression vector designated zzTev80N. The clone was kindly provided by the group of Prof. Dr. Dirk Görlich (Heidelberg). It has the ampiciline resistance gene (*bla*), an N-terminal zz-tag followed by a Tev protease restriction site, and a C-terminal His-tag.

Toc159 G and M domains were cloned into pProEX HTa: the vector and the *Pisum sativum* Toc159 amplified by PCR were restricted with EcoRI and SalI endonucleases, followed by ligation and transformation into *E. coli* DH5 α . PCR primers used for cloning are given in the Table 2.1.

Table 2.1: Primers used for PCR amplification and cloning of *Arabidopsis thaliana* Toc159 M and G domain. Capital letters in the sequence denote the part hybridizing to the gene, small letters are the restriction site and extra bases for spacing and alignment in the correct frame.

Primer	Designation	Sequence
G-domain forward	ps159-G1fw_EcoR1	cgagaattcGACTCTGATGAAGAAGATGTATC
G-domain backward	ps159-Gbw_SalI	cgagtcgacGTTAGTAGCCTCAGAGAGAATC
M-domain forward	ps159-M1fw_EcoR1	cgagaattcTTTAAACCTCTAAAGAAGTCG
M-domain backward	ps159-Mbw_SalI	cgagtcgacATAGATGGAATAGTTTTTCAGTAACA

After transforming *E. coli* BL21 cells with the appropriate construct, a single colony was transferred into 4 ml 2 \times YT medium and incubated at 24–37°C over night. The main culture was then inoculated and grown at 37°C to the OD_{600nm} of 0.6, then induced with 1 mM IPTG (0.6 mM for pProex HTa) and transferred to the optimal temperature for expression (and cooled down on ice during the addition of IPTG if the temperature for expression was below 37°C). After incubating for the time required for the expression, bacteria were pelleted and the medium was completely removed. Such bacterial pellets were stored at –20°C or immediately used for protein purification.

Unless otherwise noted, his-tagged proteins were purified using Ni-NTA column material according to manufacturer’s recommendations for denaturing purification.

2.2.2 Lipid and liposome methods

Liposome preparation

Liposomes with outer or inner envelope lipid content (see Table 2.2, data from [12]) were prepared as follows. The lipids were mixed in a glass tube to yield the final amount of 5 μ mol total

Table 2.2: Lipid composition of chloroplast envelope membranes of spinach (*Spinacea oleracea*) according to Bruce [12]. All values are in mol%.

Lipid	Outer envelope	Inner envelope
Monogalactosyldiacylglycerol	17	49
Digalactosyldiacylglycerol	29	30
Sulfoquinovosyldiacylglycerol	6	5
Phosphatidylcholine	32	6
Phosphatidylglycerol	10	10
Phosphatidylinositol	6	0

lipid content and dried under nitrogen flow. The lipids were dissolved in 1 ml chloroform followed by nitrogen drying and complete removal of the organic solvent under vacuum for at least 3 hours. The prepared lipid film was then either stored at -80°C under argon or directly dissolved in buffer S (50 mM Hepes/KOH pH 7.6, 0.2 M sucrose, degassed using N_2) for preparation of liposomes S or in buffer N (50 mM Hepes/KOH, 125 mM NaCl, degassed) for preparation of liposomes N. The solution was vortexed and subjected to five freeze/thaw cycles. Resulting multilamellar vesicles were extruded 25 times through a polycarbonate filter (Avestin, Inc., Ottawa, Canada) with the pore size of 400 nm mounted on the mini extruder (Liposofast; Avestin, Inc., Ottawa, Canada) in order to prepare unilamellar liposomes [64].

Cytochrome C loaded vesicles

For loading with cytochrome C, Buffer N, Buffer S and Buffer G (50 mM Hepes/KOH, 70% glycerol, degassed) were supplemented with 1 mM cytochrome C (final concentration) before liposome preparation in 500 μl of the indicated buffer (10 mM lipids final). After extrusion, the liposomes were purified over a 10 ml G25 size exclusion chromatography column. The liposomes were diluted to 1 mM final lipid concentration. 0.1 ml was pelleted by centrifugation at $50,000 \times g$ for 30 min at 4°C through an appropriate buffer to determine initial leakage. The supernatant and the pellet were analyzed for cytochrome C content. The remaining solution was overlaid with argon and kept at 4°C for 30 days followed by separation of the incorporated and released cytochrome C. Liposome sedimentation was confirmed by the lipid analysis of the supernatant and the pellet.

Separation of lipid sheets

Liposomes S were prepared as described using a polycarbonate filter with 400 nm pore size for extrusion. 200 μ l of this preparation were diluted with 100 μ l buffer N to reduce density of the solution. Diluted liposomes were loaded on top of 1 ml buffer S (representing the sucrose cushion) and centrifuged at $50,000 \times g$ for 30 min at 4°C. Fractions were collected as follows: top 400 μ l, middle 800 μ l, bottom 100 μ l. The fractions were analyzed by thin layer chromatography and freeze-fracture electron microscopy.

Lipid extraction and analysis

The volume of the sucrose cushion fractions was adjusted to 2 ml. The diluted fractions were mixed with 8 ml of chloroform and vortexed. Addition of 4 ml of methanol was followed by vigorous mixing. After incubation on ice for 5 min, 24 ml of chloroform:water (1:1 v/v) were added and the mixture was centrifuged for 15 min at $3,000 \times g$ at 4°C. The chloroform phase was separated and dried under nitrogen. Lipid films of the first two fractions were dissolved in 20 μ l chloroform and those of the pellet fraction in 200 μ l chloroform. 2 μ l of each fraction were spotted on 10 \times 10 cm silica gel 60 plates along with 2 μ g of standard plant lipids. Thin layer chromatography was then performed using the following systems as the mobile phase: acetone, benzene and water (45:15:4); chloroform, methanol and water (65:25:4); chloroform, acetone, methanol, acetic acid and water (10:4:2:2:1) (all proportions are by volume). The lipids were stained using 0.54 M H₂SO₄, 5.5 mM KMnO₄, 36 mM FeSO₄·7H₂O and visualized by heating at 110°C for 10 min.

2.2.3 Analytical and visualisation methods

Electron microscopy

For negative staining, the standard liposome preparation was diluted fivefold with buffer S and adsorbed on carbon-coated copper grids for 3 minutes. Upon adsorption, excess solution was blotted off with filter paper and the sample was stained with 1% (w/v) uranyl acetate for 60 seconds. For freeze-fracture, sucrose cushion fractions top and bottom were examined. The top fraction was concentrated by centrifugation at $256,000 \times g$ for 24 h at 4°C. Samples were frozen in liquid ethane, fractured and shadowed unidirectionally with Pt/C at the angle of 35° at -170°C. Samples were examined in a JEOL 100CX transmission electron microscope. Images were recorded at the magnification of 20,000 \times .

Dynamic light scattering

Dynamic light scattering (DLS) measurements were performed at 20°C in 8 mm cylindrical cuvettes at the angle of 90°. An AXIOS-150 (Triton-Hellas) apparatus equipped with a 35 mW vertically polarized diode laser operating at the wavelength of 658 nm has been used, together with a digital correlator with 288 exponentially spaced channels, spanning delay times from 11.62 ns to 56 min. Spectra were recorded every 30 s for 10 minutes. The distribution function was recovered using Provencher's regularized Laplace inversion CONTIN algorithm [78, 79]. The theory, technique and methods of determination of particle size distributions by dynamic light scattering are described in more detail in [32, 74, 92].

Absorption spectroscopy

Spectra from 400 nm to 700 nm were measured using the Shimadzu UV-2401PC spectrophotometer at room temperature with the step size of 1 nm. Measurements were conducted in semi-micro cuvettes with 10 mm optical pathway (Sarstedt, Nümbrecht, Germany). Liposomes were diluted with buffer S and incubated with detergents when appropriate.

2.2.4 Biochemical methods

Soluble leaf extract isolation

Soluble leaf extract was isolated following the published protocol [37] with the exception that a 300,000 × g or 600,000 × g centrifugation was performed as the final step.

Coimmunoprecipitation

Outer envelope vesicles were solubilised by incubation with 1.5% DeMa, 25 mM HEPES/KOH pH 7.6, 150 mM NaCl for 5 min at 20°C. Undissolved particles were removed (100,000 × g, 10 min, 4°C) and the supernatant was diluted 10 times in IP buffer (25 mM HEPES/KOH pH 7.6, 150 mM NaCl, 0.2% DeMa) including 0.05% egg albumin. After the addition of 15 ml antiserum to the mixture, the sample was incubated for 1 h at 20°C, followed by incubation with 50 ml in IP buffer pre-equilibrated protein-A sepharose (Amersham Bioscience, Freiburg, Germany) for 1 h at 20°C. After washing with IP buffer, the bound protein was eluted by cooking in SDS-PAGE loading buffer [63]. The eluted fractions were separated by SDS-PAGE and subsequently transferred to a nitrocellulose membrane and immunodecorated with the indicated antisera. The coimmunoprecipitation of soluble cell extract fractions was conducted as outlined above.

Protein amount in envelopes

Defined amounts of purified proteins or proteins present in the envelopes or organelles were separated by SDS-PAGE, blotted and incubated with primary antibodies. Primary antibodies raised against his-tagged proteins were preincubated with his-tagged pSSU, which was sufficient to remove the subset of antibodies specific for the his-tag epitope. Proteins were visualised by alkaline phosphatase staining and proteins were quantitated after scanning of blots using AIDA image analysis software. Expressed protein dilution series served as a standard for comparison with envelope/chloroplast/amyloplast bands thus enabling protein amount determination in those samples.

Toc complex isolation

The Toc complex was isolated as in [90], unless noted otherwise. Briefly, purified outer envelope of pea chloroplasts was pelleted at $200,000 \times g$ for 10 min at 4°C and resuspended in 300 μl of 25 mM Hepes/KOH, 100 mM NaCl and 1.5% n-decyl- β -D-maltoside, pH 7.0. After 10 min, the solubilized outer envelope was layered on top of a 25–70% (wt/vol) sucrose gradient (in 25 mM Hepes, 100 mM NaCl, and 0.075% n-decyl- β -D-maltoside, pH 7.0) and centrifuged for 4 h at $320,000 \times g$ at 4°C using a swinging bucket rotor. The fractions containing the Toc complex of at least six gradients were pooled, diluted four times using 25 mM Hepes, 100 mM NaCl, pH 7.0, and incubated with lipase VII for 30 min at 4°C before layering on top of a step gradient. The step gradient was composed of 25%:45%:55%:70% (wt/vol) sucrose in 25 mM Hepes, 100 mM NaCl and 0.075% n-decyl- β -D-maltoside, pH 7.0. After centrifugation for 16 h at $280,000 \times g$ at 4°C , complex fractions were collected and pooled. The isolated complex was frozen in liquid nitrogen and stored at -20°C .

The isolated complex-containing fractions were quite dilute, and when necessary they were concentrated by centrifugation at $270,000 \times g$ for 24 h at 6°C over a 70% sucrose cushion. Amounts in the range of around one microgram Toc complex could be recovered from the sucrose cushion in a typical run with 12 ml of diluted gradient fractions.

Glycerol gradients

Step gradients with 20, 25, 30, 35, 40, 50, and 70% glycerol in 20 mM Hepes pH 7.6, 125 mM NaCl and 0.1 mM MgCl_2 were overlaid with 400 μl sample and centrifuged for 2 hours at 4°C at $60,000 \times g$. Gradients were prepared in 5 ml tubes for S52-ST rotor for Sorvall Discovery™ M150 SE ultracentrifuge, each step consisting of 500 μl solution.

2.2.5 Gene chip analysis

RNA was extracted from four week old wild type *Arabidopsis thaliana* and gene chip analysis of Affymetrix ATH1 arabidopsis genome chip (Affymetrix, High Wycombe, United Kingdom) was performed according to the manufacturer's recommendation. Expression data were analysed using the software provided by Affymetrix (MAS). The data for the diurnal gene expression were downloaded from (<http://affymetrix.arabidopsis.info/narrays/experimentpage.pl?experimentid=60>). The expression values of investigated gene products were normalised according to the highest expression observed. Then the difference of expression was calculated for all combinations of transcripts at each time point and the absolute values of the differences were added.

Chapter 3

Results

3.1 Liposomes as a tool for complex investigation

Initial reconstitution procedures were developed for uniform insertion even if it meant a low reconstitution yield. For further mechanistic studies, the insertion rate of the complex had to be enhanced. In order to define efficient reconstitution protocols, several questions had to be addressed. The stability of liposomes against lysis was investigated in different buffer solutions. Due to the inclusion of outer envelope non-bilayer lipids in most of the liposome preparations, their successful incorporation into vesicles had to be confirmed. Dependence of the size of liposomes extruded through a polycarbonate filter on the filter pore size was also investigated and confirmed. Since certain reconstitution protocols and approaches depend on the exact solubilization state of liposomes, this issue had to be addressed as well. Finally, many activity assays require the knowledge of the liposome size. Although dynamic light scattering and freeze-fracture electron microscopy are widely used for size determination, they are not always available. Therefore, a method was developed in which absorption spectroscopy could replace dynamic light scattering measurements to give an estimate of liposome dimensions.

3.1.1 Liposome stability

One of the main questions for experimental approaches is the stability of liposomes after reconstitution. This stability is dependent on the lipid content of the liposomes and the buffer system used. Therefore, the stability of the liposomes composed of plant lipids in the ratio as they occur in the outer envelope of spinach chloroplasts was investigated. For that, cytochrome C was encapsulated into the liposomes. To determine its release, the absorption spectrum of cytochrome

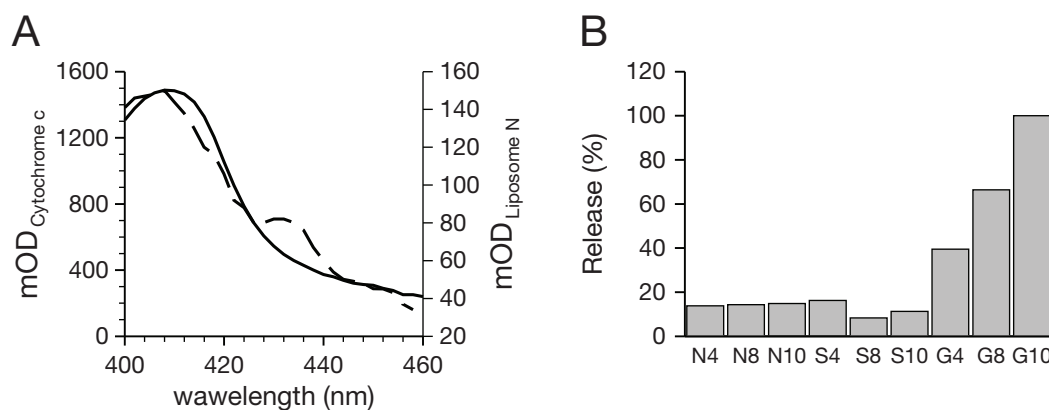


Figure 3.1: Stability of liposomes in different buffer conditions. (A) Absorption spectrum of cytochrome C (left scale, solid line) and cytochrome C encapsulated into liposomes composed of the lipid composition of the outer envelope of chloroplasts (right scale, dashed line) in buffer N. (B) Release of cytochrome C from liposomes (1 mM final concentration) after 30 days of incubation at 4°C assayed as described in Materials and Methods. Liposomes were produced in 125 mM NaCl (N), 200 mM sucrose (S), or 70% glycerol (G) with a filter of 400 nm (4), 800 nm (8) or 1000 nm (10).

C in solution was compared to the absorption spectrum of molecules enclosed in lipid vesicles (Fig. 3.1). Here, a slight difference between the two spectra has been observed. However, the maximum was found at about 406 nm in both cases. Therefore, the release of cytochrome C was determined by detection of the absorption $\Delta A_{406-460}$. Then, liposomes were created under three different buffer conditions. First, liposomes were extruded in the ionic buffer N containing 125 mM NaCl. Cytochrome C release of about 15% was observed independent of the filter size (Fig. 3.1 B; N4, N8, N10) after 30 days of incubation at 4°C. Next, sucrose of the same osmolarity (200 mOsm/kg) as the buffer N was tested. Here, a similar behavior was observed, between 10–15% of total cytochrome C was released independent of the size of the liposomes (Fig. 3.1 B; S4, S8, S10). This points to the conclusion that the ionic strength has no influence on the liposome stability, even though ionic lipids are present in the mixture. Stability of liposomes in 40% (not shown) or 70% glycerol was also analyzed. Here, a drastic difference in stability has been observed. For both concentrations a clear dependence on the liposome size was evident (Figure 3.1 B; G4, G8, G10) (see above). Liposomes prepared with the 400 nm filter released about 40% of the encapsulated cytochrome C (Fig. 3.1 B; G4), whereas liposomes prepared with the 1000 nm filter were completely depleted of cytochrome C (Figure 3.1 B; G10). Almost no lipids could be detected in the pellet when liposomes were prepared in glycerol, whereas in the other cases no lipids could be determined in the supernatant (not shown). This suggests that lipo-

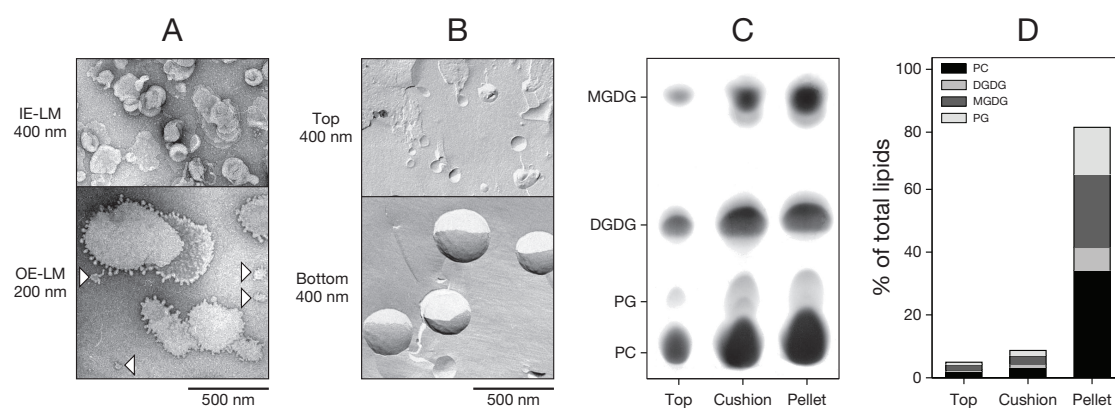


Figure 3.2: Liposome analysis. (A) Electron micrographs of negatively stained samples containing 400 nm inner envelope liposomes (upper panel) and 200 nm outer envelope liposomes (lower panel). Arrowheads indicate suspected lipid sheets. (B) Freeze–fracture electron micrographs of fractions from 400 nm liposomes centrifuged over a sucrose cushion. The upper panel shows lipid sheets and small liposomes in the top fraction, and the lower panel shows liposomes of uniform size, devoid of lipid sheets, collected in the bottom fraction. (C) Lipids of the top (left lane), the cushion (middle lane), and the pellet (right lane) of the sucrose gradient after separation were extracted and separated as described. (D) Lipid content of the three fractions was quantified and normalized to the total amount of lipids. MGDG, monogalactosyldiacylglycerol; DGDG, digalactosyldiacylglycerol; PG, phosphatidylglycerol; PC, phosphatidylcholine.

somes created in 40% or 70% glycerol are unstable and should always be prepared fresh. Such liposomes can be stored up to two days, since significant leakage was observed only after this time (not shown).

3.1.2 Liposome size determination by dynamic light scattering and electron microscopy

For obtaining liposomes of a defined size extrusion through a polycarbonate filter is very often the method of choice. For standard lipid compositions the size was found to be almost linearly dependent on the pore size of the polycarbonate filter [64]. However, lipid composition of chloroplast envelope membranes includes galactosyldiacylglycerol derivatives, which might alter the behavior during extrusion. Therefore, two lipid compositions were analyzed, namely the composition of the outer and of the inner envelope of chloroplasts (Table 2.2). The most significant difference between these two compositions is the drastic increase of the non-bilayer lipid monogalactosyldiacylglycerol (MGDG) from 17% to 49%. In order to determine the size and shape of the liposomes, the samples were initially analyzed by negative staining electron microscopy (Fig. 3.2 A). The analyses have shown that the inner envelope lipid mixture (IE-LM) yields li-

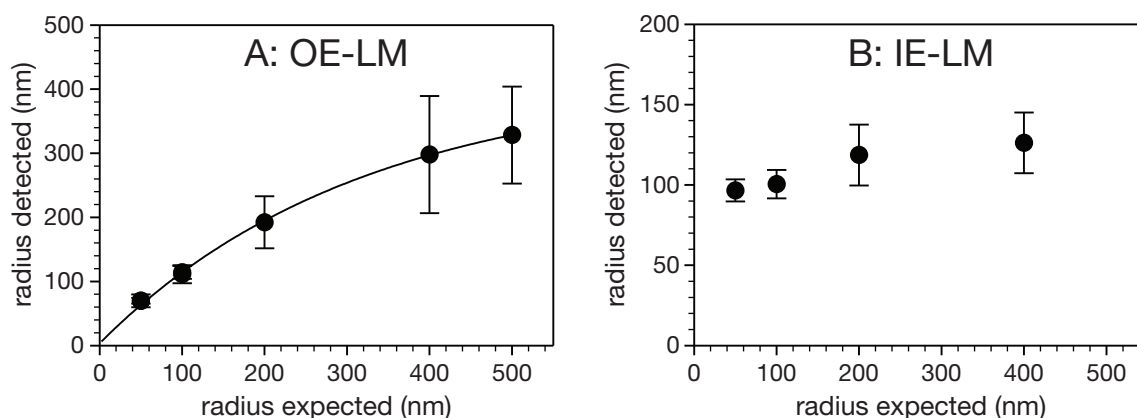


Figure 3.3: Liposome size determination by DLS. Liposomes with the outer envelope lipid composition (A) and inner envelope lipid composition (B) were produced using polycarbonate filters of different sizes (radius expected). The size was determined by DLS as described. Error bars indicate the standard deviation observed.

liposomes that are smaller than expected (Fig. 3.2 A, upper panel). For the outer envelope lipid mixture (OE-LM), liposomes were in the expected size range, but we suspected the formation of lipid sheets (Fig. 3.2 A, lower panel, arrows). To confirm this conclusion samples of both compositions were analyzed by freeze-fracture EM, since negative staining often produces drying artifacts (Fig. 3.2 B). Here, the size of the liposomes with outer envelope lipid composition (Fig. 3.2 B, lower panel) agrees with the size determined by dynamic light scattering.

When liposomes were re-purified by centrifugation through a sucrose cushion, the pellet was free of lipid sheets, as determined by electron microscopy (Fig. 3.2 B, lower panel), whereas in the supernatant fraction only lipid sheets or very small liposomes were detected (Fig. 3.2 B, upper panel). Since the investigated lipid mixtures included non-bilayer lipids, the lipid content of the suspected lipid sheets was analyzed. Lipid compositions of the top layer (representing the lipids that did not enter the cushion), the cushion itself and the pellet were analyzed. All the fractions had the same lipid composition (Fig. 3.2 C). When the lipid content was quantitated, 20% of the lipids were present in the supernatant and 80% in the pellet (Fig. 3.2 D). Therefore, liposomes and their corresponding lipid sheets have identical composition. Furthermore, only a small proportion of the lipids has been found in the sheets.

Next, liposome size was analyzed by dynamic light scattering. For the liposomes with the outer envelope lipid composition the size did not linearly depend on the pore size of the polycarbonate filter (Fig. 3.3 A). For example, liposomes created with a filter of the pore radius of 400 nm revealed an average size of the liposomes with radius of about 300 nm. Furthermore, as the liposomes become larger, the observed liposome size range also increases. When the inner

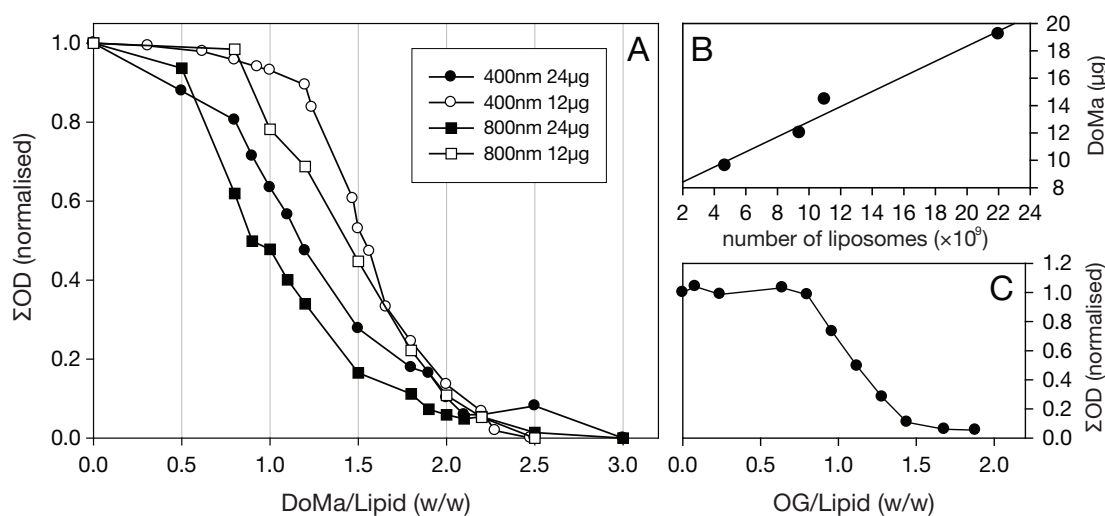


Figure 3.4: Liposome solubilization by dodecylmaltoside (DoMa) and octylglucoside (OG). (A) Liposomes composed of a lipid mixture reflecting the chloroplast outer envelope composition were extruded through a polycarbonate filter of the pore size of 400 nm (circles) or 800 nm (squares) and were diluted to the final lipid concentration of 24 $\mu\text{g}/\mu\text{l}$ (closed symbol) or 12 $\mu\text{g}/\mu\text{l}$ (open symbols). The liposomes were solubilized with DoMa using the indicated amount of detergent (given as a ratio to the lipid concentration). Optical density was measured in the range between 400 and 700 nm in 1 nm steps, and the optical densities for the wavelengths were added up and normalized to the value without DoMa addition (ΣOD (normalised)). The values were plotted against the ratio of DoMa and lipid (weight/weight). (B) The amount of DoMa required for onset of solubilization. The number of liposomes was calculated according to the determined liposome size (Fig. 3.3 A) and the lipid concentration and was plotted against the DoMa concentration used. (C) Shown is the solubilization of 24 μg of liposomes constructed using the polycarbonate filter with the pore size of 400 nm by OG as described for the same procedure in (A) as a representative result.

envelope composition was used, no dependence on the filter size used has been observed. All the liposomes had an average radius of 100–120 nm, regardless of the filter pore size (Fig. 3.3 B).

3.1.3 Liposome solubilization

Many protocols for reconstitution of proteins into preformed liposomes require partial solubilization of the preformed liposomes [83]. In the previously described protocol, liposomes were solubilized by octylglucoside [88]. Solubilization by this detergent took place when lipid to detergent ratio was 1:1 (w:w), which is in line with other results [73] (Fig. 3.4 C), suggesting that the lipid composition did not have a major influence on the solubilization behavior. Furthermore, no dependence on the liposome size has been observed (not shown). In contrast, analysis of the solubilization of liposomes by dodecylmaltoside revealed a clear dependence of this ratio on

the amount of the lipid added (Fig. 3.4 A, compare corresponding black and white symbol) and on the liposome size (Fig. 3.4 A, compare circles and squares). Therefore, the amount of this detergent necessary for partial solubilisation is dependent on another parameter than the lipid concentration as long as the authentic outer envelope lipid mixture is used. Taken together, lipid amount and liposome size could be interpreted as number of liposomes. Analysis of the obtained solubilization concentration revealed a clear dependence on the number of liposomes (Fig. 3.4 B). This could be explained by the fact that solubilization takes place upon interaction between detergent micelles and liposomes. Since the exact onset of liposome solubilization, when the liposomes are saturated with detergent but have not yet started to dissolve, represents a very important point for some reconstitution protocols, the relationship between liposome number and mass of the added detergent was investigated. Analyzing the relationship by linear regression revealed the following relation: in order not to solubilize a given number of liposomes, the amount of the detergent should not exceed the amount in μg ($mDet$) given by the formula:

$$mDet = 7.3DoMa + 0.55DoMa \cdot \frac{N(liposomes)}{10^9}$$

where $DoMa$ is the mass of dodecylmaltoside in μg , and $N(liposomes)$ the number of liposomes. Following this rule, it will now be possible to calculate the point of the onset of solubilization, which in turn makes design of a certain type of new reconstitution protocols for outer envelope proteins possible.

3.1.4 Determination of liposome size by absorption spectroscopy

In order to use dodecylmaltoside as the solubilizing detergent, it is necessary to estimate the liposome number which is directly dependent on lipid concentration and liposome size. The size of the generated liposomes is dependent on the lipid ratio used, as shown by Fig. 3.3. However, for many approaches it is necessary to know the liposome size after the reconstitution procedure. Therefore, the next step was to find out whether dynamic light scattering could be replaced by simple absorption spectroscopy for size determination. Absorption (turbidity) in the visible light wavelength range from 400 to 700 nm had been analyzed in 1 nm steps. The observed absorption value for each wavelength was added up and the corresponding value was plotted against the lipid concentration (Fig. 3.5 A). A linear dependence of the 'integrated' optical density on the concentration of lipids and also on the amount of liposomes could be determined (Fig. 3.5 A). Furthermore, liposomes of different sizes did not follow the same linear dependency. Analysis of the dependence of the slope of the linear regression of individual relationships between lipid

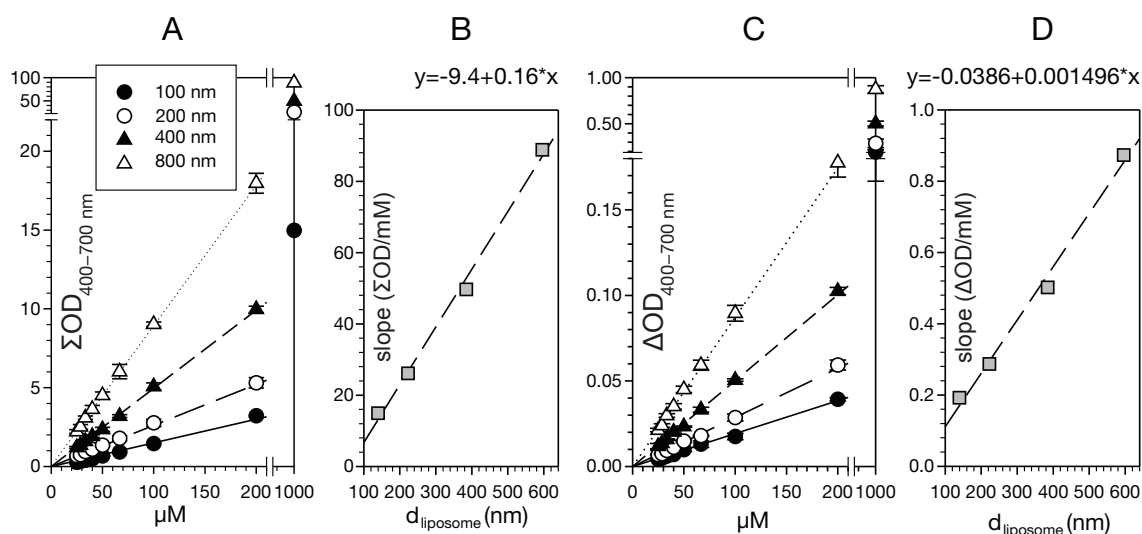


Figure 3.5: Liposome size determination by absorption spectroscopy. (A) The absorption spectra of liposomes created with a polycarbonate filter of indicated pore size with a defined lipid concentration were measured in the range between 400 and 700 nm in 2 nm steps, and the optical densities for the wavelengths were added up. Lines represent the linear regression to the corresponding values of one liposome size. Legend values indicate the filter pore diameter. (B) The slope of the linear regression shown in (A) was plotted against the determined liposome size (Fig. 3.3 A). The dashed line represents linear regression, and its equation is written above the graph. (C) and (D) are analogous to (A) and (B), respectively, but the ΔOD value is presented in place of ΣOD .

concentration and the optical density and the determined liposome size (Fig. 3.3) revealed a linear dependence as well (Fig. 3.5 B). This linear relation cannot be explained by a dependency on the liposome number but indicates that scattering intensity increases with radius of the particle. Therefore, knowing the lipid concentration in a sample, it is possible to determine the liposome size by measuring the absorption at two different concentrations. The same is true for analysis of the difference of the absorption (turbidity) at 700 and 400 nm (Fig. 3.5 C, D), where the slope of absorption decay is size and concentration dependent. This would be a rather simple method to give an estimate of the liposome size without the need for a light scattering facility. However, after the procedure of reconstitution of proteins into liposomes the lipid concentration cannot be simply estimated from the concentration initially used. Hence, either the lipid concentration has to be determined chemically and the liposome size can be estimated by the suggested technique or the average size can be determined by dynamic light scattering and the lipid concentration can be estimated by using the determined slope. However, a relatively large portion of the reconstituted sample, amount of which is usually limited, would have to be sacrificed for such measurements.

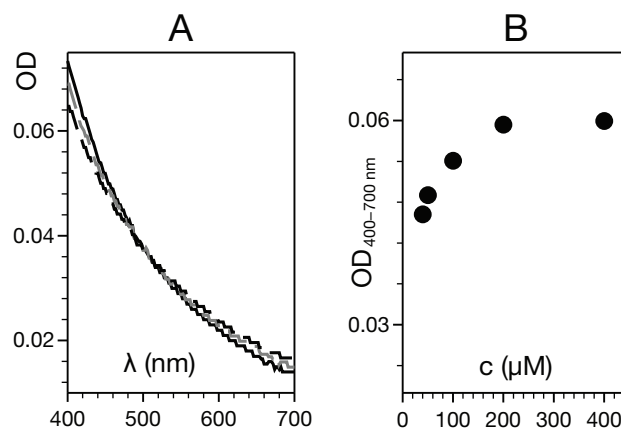


Figure 3.6: (A) The absorption spectra of liposomes created with a polycarbonate filter with 200 nm (solid), 400 nm (gray dashed), and 800 nm (dashed) pore diameters, with the concentration revealing $\Sigma\text{OD} = 5.08$ in the range between 400 and 700 nm, is shown as an example. (B) For liposomes of different sizes, the concentration was adjusted to obtain $\Sigma\text{OD} = 5.08$. Subsequently, the ΔOD in dependence on the lipid concentration is shown.

Analysis of the slope of the absorption curve of different liposomes that have the same ‘integrated’ optical density (Fig. 3.6 A) revealed a different shape for different liposome size. The difference of the absorption value at 400 nm and 700 nm shows an exponential behavior in relation to the lipid concentration (Fig. 3.6 B). Taking into account that the determined liposome size is in the range of 100–800 nm in diameter, the classical scattering theory cannot be applied any longer to describe the absorption spectra. The absorption is now dependent on the radius of the particle [52, 110]. Small particles, e.g. Rayleigh scatterers have a scattering intensity proportional to r^6 . For larger particles ($r > \text{wavelength}/20$), the form of the particle influences the scattering intensity. For haze, the geometric cross section was determined [52], and can be described in the range of interest by equation E8, section 3.1.5. In turn, representation of the value in dependence of the wavelength normalized to the geometric radius of the particle (Fig. 3.7 A, white circles) can be described, in the range of interest, by equation E9. However, to compare the data obtained here with the geometric cross section, the values have to be corrected for the gyration radius (Fig. 3.7 A, grey circles). Hence, an overlay of the optical density determined in relation to the normalized wavelength with the geometric cross section demonstrates that the determined relation can describe the observed behavior (Fig. 3.7 B). Analyzing the difference between the absorption value at 400 nm and at 700 nm in relation to the concentration defining parameter (equation E7, see below) for different constant integral values according to equation E11, (see below) shows the same behavior as determined for the liposomes (compare Fig. 3.6 B

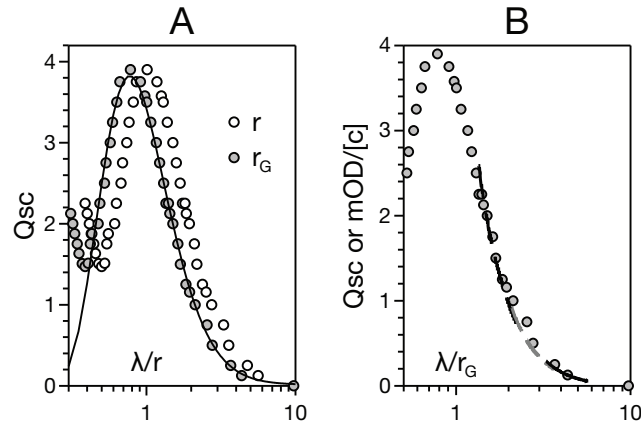


Figure 3.7: (A) Values taken from Klassen [52] (white circles) were adjusted to the gyration radius (gray circles). The line represents the least squares fit to equation E9. (B) Overlay of the values from (A) with the values from Fig. 3.6 A normalized according to the lipid concentration.

and Fig. 3.8 A). This supports the notion that scattering behavior of the prepared liposomes can be described by the geometric cross section as previously established [52]. Hence, two independent parameters are available for analysis of the liposome size and concentration by absorption spectroscopy by determining the out scattering.

Data analysis

A calibration plot of liposome diameter vs. $\Sigma OD/\Delta OD$ was constructed, and least square fit of either a hyperbolic or an exponential function was performed (Fig. 3.8). The hyperbolic function used has the general form

$$y = y_0 + \frac{x + c}{a + b \cdot (x + c)} \quad (\text{E1})$$

the parameters being $y_0 = 60.01$, $a = 0.815$, $b = 0.022$, $c = -128.8$. The correlation was $r^2 = 0.99994$. The exponential function was

$$y = y_0 + a \cdot [1 - e^{-b \cdot (x+c)}] \quad (\text{E2})$$

with the parameters $y_0 = 67.9$, $a = 33.597$, $b = 0.015$, $c = -137$. The correlation was $r^2 = 0.9962$.

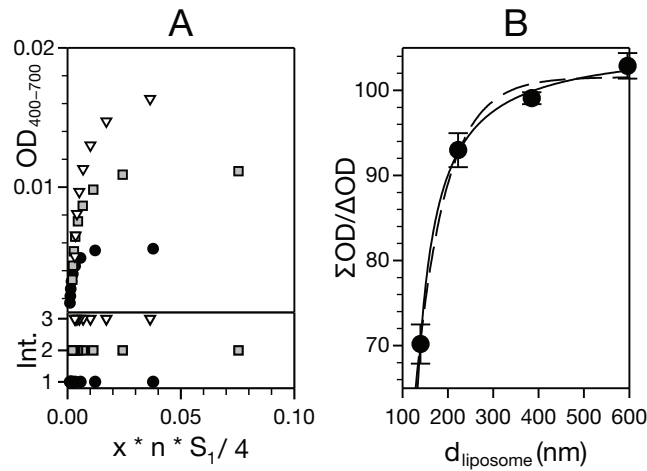


Figure 3.8: (A) For the integral values of 1, 2, and 3 according to equation E11 (lower panel), the difference of the two extreme absorption values in dependence of $x \cdot n \cdot S_l/4$ representing the concentration is shown (upper panel). (B) The concentration-independent relation between liposome size and the ratio of ΣOD to ΔOD is shown. The solid line represents the least squares fit of a hyperbolic function (equation E1), and the dashed line represents the least squares fit of an exponential function (equation E2).

3.1.5 Theoretical explanation

Classical description of scattering fails to provide an adequate framework needed to describe and explain the measurements in section 3.1.4. Therefore, a new theoretical model had to be constructed.

Determination of the absorption of liposomes takes into account two phenomena: the absorption of light by lipids and the out-scattering effects [52, 110]. However, for the investigated liposomes ($r \approx \lambda$), the out-scattering effects alone can describe the measured absorption. In general, the total amount of light scattered by an individual particle per unit incident irradiance can be described by scattering cross section $\sigma_{SC}(\lambda)$, which is wavelength dependent. Scattering efficiency is, however, defined as the ratio of the scattering cross section and its geometric cross section ($Q_{SC} = \sigma_{SC}(\lambda)/2\pi r^2$) and, therefore, is wavelength dependent as well. Absorption is defined as

$$A(\lambda) = \lg \frac{I_0}{I} = \varepsilon \cdot c \cdot x = 2.303 \cdot \alpha \cdot x \quad (\text{E3})$$

where x is the dimension of the sample, c is the concentration, ε is the molar absorption coefficient, and $\alpha (= 2.303 \cdot \varepsilon \cdot c)$ is the absorption coefficient. α can be expressed as

$$\alpha = N \cdot \sigma_{SC}(\lambda) = N \cdot Q_{SC}(\lambda) \cdot 2\pi r^2 \quad (\text{E4})$$

where N is the density of particles (or particles per unit volume), $\sigma_{SC}(\lambda)$ is the absorption cross section, and $Q_{SC}(\lambda)$ is the geometric cross section [52]. Using equation E4, the equation E3 can be rewritten as

$$A(\lambda) = 2.303 \cdot x \cdot N \cdot Q_{SC}(\lambda) \cdot 2\pi r^2 \quad (E5)$$

The density of particles is also dependent on the lipid concentration and the liposome size:

$$N = n \cdot \frac{S_l}{8\pi r^2} \quad (E6)$$

where, n is the number of lipids per unit volume (lipid concentration) and S_l is the occupied surface per lipid. Therefore, equation E3 can be transformed into

$$A(\lambda) = 2.303 \cdot x \cdot n \cdot S_l \cdot \frac{Q_{SC}(\lambda)}{4} \quad (E7)$$

From equation E5, it becomes obvious that the absorption spectra obtained for a certain liposome class depend on the scattering efficiency only. Analyzing the curve presented by Klassen [52] for haze as the model, the empirical description of this oscillation is

$$Q_{SC} = y_0 + a \cdot e^{-r/\lambda^d} \cdot \sin(b \cdot r/\lambda + c) \quad (E8)$$

However, this equation does not reveal an analytical solution of the integral required to describe the analysis presented. Inverting the presentation to λ/r allows us to describe the results by

$$Q_{SC} = y_0 + a \cdot [\ln(\lambda/r) + c]^{10} \cdot e^{-b \cdot [\ln(\lambda/r) + c]} \quad (E9)$$

Therefore, equation E5 can be written as

$$A(\lambda) = 2.303 \cdot x \cdot n \cdot \frac{S_l}{4} \cdot [y_0 + a \cdot \ln(\lambda/r) + c]^{10} \cdot e^{-b \cdot [\ln(\lambda/r) + c]} \quad (E10)$$

To describe the relation of the lipid concentration presented by n to the determined integral absorption, the integral of equation E10 can be solved as follows:

$$\int_{400}^{700} A(\lambda) d\lambda = 2.303 \cdot x \cdot n \cdot \frac{S_l}{4} \cdot [300 \cdot y_0 + a \cdot \int_{400}^{700} [\ln(\lambda/r) + c]^{10} \cdot e^{-b \cdot [\ln(\lambda/r) + c]} d\lambda] \quad (E11)$$

Thereby, the term $x \cdot n \cdot S_l/4$ can be calculated for a given radius of the liposome and a given integral of the absorption. To describe the relation of the lipid concentration presented by n to

the determined difference of the absorption at 400 and 700 nm, the value $A_{400nm} - A_{700nm}$ can be calculated directly from the equation E10.

3.1.6 A proposed method for size determination

Based on the obtained results of spectrophotometric measurements and on the theoretical explanation, a method for liposome size determination is proposed. First, unilamellar liposomes with the desired lipid composition should be prepared, e.g. by extrusion through polycarbonate filters of different size. In general, verification of the liposome size by dynamic light scattering is recommended for the data used to construct a standard curve. In this case, the dynamic light scattering is used only once for the construction of the calibration curve, as opposed to its use on a regular basis for liposome size determination, which is significantly more time-consuming. Furthermore, size verification could be omitted for standard lipid compositions (i.e. no non-bilayer lipids). After unilamellar liposomes are created, their absorption spectra should be recorded and a calibration plot of liposome diameter vs. $\Sigma OD/\Delta OD$ should be created (like Fig. 3.8 B). Use of several dilutions of liposomes of each size is recommended, since it provides a more reliable data set. For curve fitting either a hyperbolic function (Fig. 3.8 B, solid line, equation E1) or an exponential function (Fig. 3.8 B, dashed line, equation E2) is recommended. The theory covers liposome diameters above 100 nm, and the choice of the function for the least square fit depends on the desired range of measurement and the calibration data set. The calibration plot can now be used for simple determination of liposome size in subsequent measurements.

Alternatively, calculations can be based on a plot of the linear dependence of the slope of ΣOD vs. $c(\text{lipids})$ or ΔOD vs. $c(\text{lipids})$ on the liposome size (like Fig. 3.5 B and D). This plot can be used for determination of liposome concentration if the size is known (e.g. from dynamic light scattering, Fig. 3.3) or for determination of liposome size if the lipid concentration is determined by other means (e.g. chemically). These are used to construct a plot of $c(\text{lipids})$ vs. ΣOD or ΔOD . Slope of either of these plots can be linearly correlated to the liposome size (see Fig. 3.5). The liposome size can be obtained from the same measurement using a plot like Fig. 3.8 B.

3.2 Toc complex isolation

For isolation of the Toc complex from outer envelope of pea chloroplasts a working protocol had already been established by [90], and could readily be used with minor modifications as described in Materials and Methods (page 18). However, large quantities of purified outer envelope were required as starting material, and the yield of this method was low even with large

Table 3.1: Properties of detergents used for systematic envelope solubilisation testing.

Detergent	Mw (kDa)	CMC (mM)	CMC (‰)	Class
n-decyl- β -D-maltoside	482.6	1.8	0.8687	main
C ₁₀ E ₉	559.1	1.3	0.7268	main
Cymal-2	452.5	120	54.3	main
Cymal-6	508.5	0.56	0.2848	main
Digitonin	1229	0.087	0.1069	additive
Pluronic F-68	8350	-	-	additive
n-dodecyl- β -D-maltoside	348.5	0.15	0.0523	additive
Octyl- β -D-glucoside	292.4	25	7.31	additive

amounts of starting material. In order to purify larger quantities of the Toc complex, possibly using chloroplasts as starting material, development of a new protocol was attempted.

Extensive detergent testing was done to find the optimal formula for envelope solubilisation. Envelope was solubilised with the indicated detergent mixture and then centrifuged on glycerol step gradients as described in Materials and Methods section (page 18), with the only difference that the run lasted 18 hours. After a preliminary testing of all detergents available in the laboratory, their selection was narrowed to those which performed satisfactory. They were then divided into two groups: main solubilising detergents and additives which help separation on the gradient. This division and initial detergent selection, as well as the initial concentration used to test solubilisation, were based on previously conducted large scale tests (Schleiff, personal communication). Preliminary solubilisation testing led to systematic testing of detergents summarized in Table 3.1. It also revealed that the solubilisation efficiency depends on CMC and micelle concentration rather than simply the concentration of detergent molecules, which leads to the conclusion that the mechanism of solubilisation of membrane vesicles is probably fusion with detergent micelles.

After systematically testing detergent combinations presented in Table 3.1, C₁₀E₉ was selected as the best main solubilizing detergent, and Pluronic-F68 as the most efficient additive. After testing different concentrations in the range from 0.1% to 3%, the best solubilizing concentrations were 2% for C₁₀E₉ and 1% for Pluronic. Pluronic concentrations of more than 1% led to poor resolution of gradients. As a possible help for solubilisation of sugar headgroups of chloroplast envelope lipids, detergents of similar structure, namely decylmaltoside and octylglucoside, have been tested in various concentrations ranging from 0.1% to 1% as possible second additives. Addition of 0.1% octylglucoside produced somewhat more uniform solubilisation and better separation on the gradient. Since the ratio of the amount of a detergent and the solubi-

lized sample represents an important parameter, it should be noted that all of the solubilisation tests have been performed using the final concentration of outer envelope of the equivalent of 0.6 $\mu\text{g}/\mu\text{l}$ protein.

Isolated outer envelope is a good starting material in terms of abundance of the Toc complex, but its use has several shortcomings. Outer envelope isolation is an expensive and labor-intensive procedure with limited yield. An even more important problem is that the purification takes several hours, during which time the structural and functional integrity of the Toc complex comes in question. Therefore, chloroplasts were tested as the starting material for solubilisation. After following the first several steps in the standard envelope isolation protocol, chloroplasts washed after Percoll gradients were mixed with one volume 1.1 M sucrose and 6 mM MgCl_2 and incubated for 10 min in darkness. This was followed by 50 strokes in a Dounce homogenizer. Two rounds of centrifugation for 5 min at $5,000 \times g$ at 4°C were sufficient to pellet most of the thylakoid system membranes. The supernatant performed similarly to the isolated envelope in terms of solubilisation and complex purification, although a concentration step would be required for a more direct comparison.

After solubilisation with the optimal detergent mixture (2% C_{10}E_9 , 1% Pluronic and 0.1% OG) and centrifugation on glycerol step gradients as described in Materials and Methods section (page 18), bulk of the Toc material could be detected near the bottom of the gradient. Therefore, preliminary purification of the Toc components containing fraction has been performed by centrifugation at $10,000 \times g$ for 20 min at 4°C . Surprisingly, most of the Toc complex has been recovered from the pellet fraction, which was resuspended in a buffer containing 20 mM Hepes pH 7.6 and 125 mM NaCl, and filtered through a filter with pores measuring 0.45 μm in diameter in order to remove crude aggregates. Since there was no significant loss of material after filtering (data not shown), the resuspended pellet was considered to be in an at least largely solubilised form and was therefore further used as a sample for glycerol gradients which were run as described above. Resulting complex-containing fractions were again collected near the bottom of the gradient; they had typical Toc core complex subunit composition and displayed GTPase activity typical for outer envelope receptors Toc34 and Toc159 (not shown).

Currently, the Toc complex can be isolated most efficiently as follows. Starting material, either outer envelope or quickly isolated mixed envelopes, can be efficiently solubilized by a mixture of detergents containing 2% C_{10}E_9 , 1% Pluronic F-68 and 0.1% OG. After 10 min of incubation, the Toc complex is pelleted by centrifugation at $10,000 \times g$ for 20 min at 4°C . The pellet is then resuspended and can be further purified by centrifugation on a glycerol gradient or by other methods (e.g. size exclusion chromatography). Although there are indications that the

Table 3.2: Toc159 was expressed in BL21(pMICO) cells at different temperatures, and the yield, stability and solubility were estimated according to staining intensities using Toc159 antibodies. Expression was correlated to the intensity of the bands (equal loading), stability to the observed proteolytic fragments, and solubility to the partition between the supernatant and the pellet after centrifugation of the bacterial lysate for 20 min at $20,000 \times g$ at 4°C . Number of symbols (●) correlates to the estimated relative value of the corresponding parameter.

Temperature	Expression	Solubility	Stability
17°C	●●	●●●	●●●
24°C	●●●	●●●	●●●
37°C	●●●●	●●●●	●

pelleted material indeed contains solubilized active Toc complex, additional research is necessary to confirm this.

3.3 Function and localization of Toc159

3.3.1 Expression of Toc159

Expression and purification of the full length Toc159 was not successful, although separately cloned domains (M and G) express in *Escherichia coli* without any difficulties. The very low level of expression of the full length protein is probably due to its susceptibility to degradation and aggregation, and its toxicity for *E. coli*. All attempts to express the full length Toc159 in an RTS 100 cell-free *in vitro* translation system (pIVEX vectors) were unsuccessful. Since this system has other drawbacks, namely high cost and low yield even when maximum expression has been achieved, the main focus was set on attempts to overexpress atToc159 in an *E. coli* system. Combination of several parameters had to be tested in attempt to achieve Toc159 overexpression: bacterial strain, helper plasmids, culture medium, expression temperature and expression duration.

Several *E. coli* strains were tested for expression yield and stability of the produced protein. Helper plasmids for codon bias correction (pMICO, pRosetta) were used in order to promote expression of eukaryotic genes in a prokaryotic system. Tight induction control provided by pMICO helps expression of proteins that are toxic for *E. coli* [22]. Properties of different strains and helper plasmids are summarized in Table 3.3.

BL21(DE3)Origami strain was completely unable to express Toc159. Top10F' strain could express a very low amount of Toc159, but the protein was badly degraded. A strange degradation

Table 3.3: *Escherichia coli* expression strains tested for the ability to overexpress the full length Toc159. Details can also be found in the Materials and Methods section, page 12.

Strain	Plasmid	Properties
BL21(DE3)	none	Routinely used <i>E. coli</i> expression strain.
BL21(DE3)Star	none	Strain with increased mRNA stability.
BL21(DE3)Origami	none	Disulfide bond isomerisation.
Top10F'	none	Another T7 promotor compatible expression strain.
BL21(DE3)/RP	pRP	Corrects for codon bias.
BL21(DE3)/RIL	pRIL	Corrects for codon bias.
BL21(DE3)/pMICO	pMICO	Corrects for codon bias and tightens induction control.
BL21(DE3)/pRosetta	pRosetta	Corrects for codon bias.
BL21(DE3)Star/pRosetta	pRosetta	Increased mRNA stability, corrects for codon bias.
BL21(DE3)Star/pMICO	pMICO	Increased mRNA stability, corrects for codon bias and tightens induction control.

pattern was also observed in BL21(DE3)/RP. Expression in these three strains was therefore not analysed further.

Remaining strains were able to express Toc159 only in a hardly detectable amount. They were compared in terms of relative yield and product stability. Protein stability was determined according to degradation products observed after western blotting and staining with primary and secondary antibodies (both termini) or secondary antibody only (zz-tag, N terminus). BL21(DE3) had properties very similar to BL21(DE3)/pMICO, but the overall yield was somewhat lower. BL21(DE3)/pRosetta performed very similarly to the equivalent “Star” strain. BL21(DE3)/pMICO “Large” was a special phenotype variation observed on some BL21(DE3)/pMICO plates: occasionally several large fast-growing colonies appeared, which exhibited distinctive expression properties—somewhat better yield while maintaining protein stability, when compared to ‘normal’ BL21(DE3)/pMICO. This variation had been observed several times on plates with freshly transformed BL21(DE3)/pMICO cells. Although the observed phenomenon could be the result of a mutation in the Toc159 gene, the underlying cause was not investigated further—instead, these bacteria were treated as a separate strain. “Star” cells had lower stability of the expressed protein than BL21(DE3)/pMICO, and were not tested further despite somewhat better yield.

Considering the relative yield and atToc159 stability, BL21(DE3)/pMICO strain had the best expression profile: while producing relatively non-degraded protein, the yield was comparably high. Although the optimal strain was identified, absolute amount of the expressed protein in a typical overexpression (1 l) was dedectable only by western blotting (Fig. 3.9 A). BL21(DE3)/pMICO “Large” variety seemed a promising alternative because it grew faster and produced

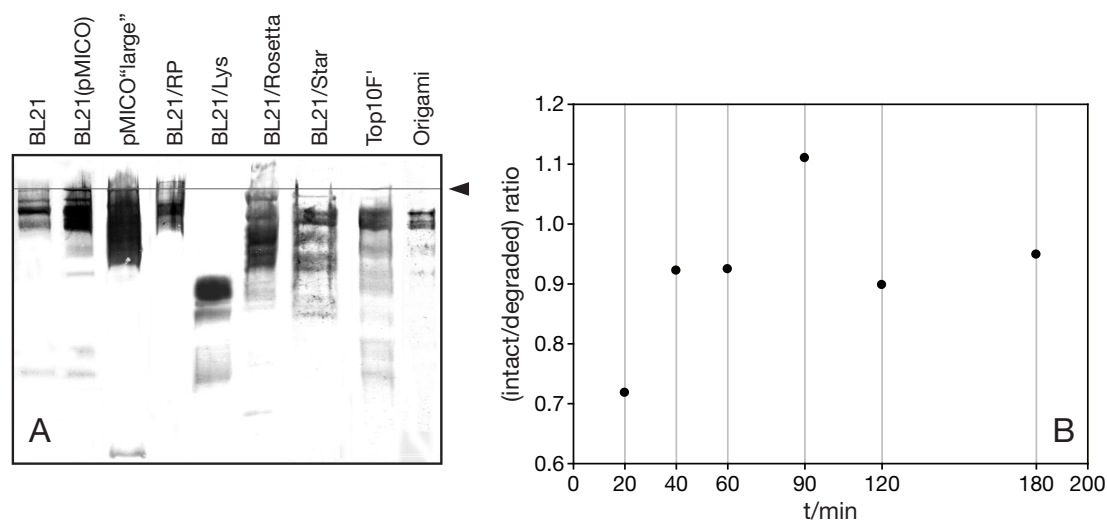


Figure 3.9: Optimization of Toc159 expression. (A) Western blots of test expression in different *E. coli* strains. Corresponding strain is indicated above each lane. Intensity corresponds to the amount of the expressed protein, and the stability can be estimated from degradation products. Arrowhead on the right side and the thin grey line across the blot indicate size of the full length protein. (B) Ratio of intact and degraded expressed Toc159 after different expression time (one experiment). After 90–120 min product accumulation stops, and degradation takes over. Protein amounts were estimated by quantitation of western blots.

more protein. There is, however, one major drawback—the unknown mechanism or mutation that produces this peculiar phenotype has not been explained.

2×YT medium was routinely used for overexpression. Other media were tested to ascertain whether their nutrient composition alters the yield or stability significantly. The main focus was on the M9ZB minimal medium and 2×YT with 2% glucose or glycerol, because these may influence induction properties and therefore alter expression of toxic proteins. Tested media included 2×YT, 2×YT with 2% glucose, 2×YT with 2% glycerol, TB and M9ZB minimal medium. Media were tested by varying both expression temperature and *E. coli* strain along with the nutrient composition. No significant difference was observed, even between very different media (i.e. 2×YT and M9ZB). Therefore, 2×YT was selected for further experiments because it is a rich medium that enables fast growth.

Different temperatures have been shown to affect stability and solubility of other overexpressed proteins. Therefore, temperatures of 17°C, 24°C and 37°C were compared. Temperatures were varied along with medium composition (2×YT and TB) and strain (BL21(DE3)/pMICO, BL21(DE3)/pMICO “Large”, Top10F). Yield, stability and solubility of the expressed protein were analysed in order to evaluate experimental conditions (2×YT only, Table 3.2).

Stability and solubility decrease with increasing temperature. This effect is most prominent at the 24°C to 37°C shift (Table 3.2). Yield slightly increases with temperature, which could be explained by slightly faster residual growth after induction and therefore larger final biomass. Culture medium composition had no effect whatsoever. The best combined results were obtained when temperature was around 24°C. Higher temperature (37°C) led to decreased stability and solubility of the expressed protein, but not to an extent which would be a good trade-off with the slow growth and impaired yield at 17°C.

Dependence of protein yield, stability and solubility on time was monitored in order to optimize this parameter (Fig. 3.9 B), but only for the BL21(DE3)/pMICO strain at 24°C. Expressed protein is detected very soon after induction (20 min), and continues to increase in amount until 90 min after induction. Around 120 min after induction product accumulation stops, and the later period is dominated by degradation. Solubility essentially stays at the same level for at least 120 min after induction. After 180 min solubility drops significantly. Therefore, optimal expression time is between 60 and 90 min.

Although a range of conditions had been tested, total protein purified from a 1 l expression run was barely detectable on a Coomassie stained gel. Therefore, expression of full length Toc159 remained limited to minute amounts. In contrast, M and G domain could be expressed and purified without any problem using standard methods as described in Materials and Methods.

3.3.2 Localization of Toc159

Toc159 has been reported to exist in the cytosol as well as in the outer envelope membrane. A model was proposed in which Toc 159 binds to precursor proteins in the cytosol and targets them to the membrane[37]. Because of the implication that Toc159 functions before Toc34 in the import pathway, it was important to reinvestigate this finding by following the procedure described [37]. Intact chloroplasts and cell debris were removed from the homogenate by centrifugation (500 × g). The presence of chloroplast proteins within the pellet was verified by immunoblotting (Fig. 3.10 A, lane 1). The supernatant was then subjected to ultracentrifugation (100,000 × g, 2 h). Toc159 was found in the pellet as well as in the supernatant fraction. Consistent with previously reported results [37] Toc34 was restricted to the membrane pellet (lane 2, 4). Toc64 and LHCPII were also restricted to the pellet fractions (lane 2, 4, data not shown). Surprisingly, the outer envelope proteins Oep37 and Toc75 and the inner envelope proteins Tic110 and Tic40 were present in the soluble fractions as well (lane 2, 4). Even after centrifugation at 300,000 × g for 2 h the integral membrane proteins Toc159, Toc75, Oep37, Tic110 and Tic40 partly remained in the supernatant (lane 5). This observation raised the question whether these envelope proteins

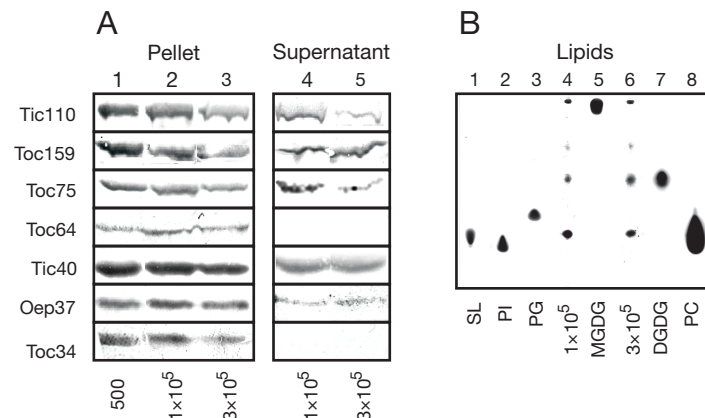


Figure 3.10: Isolation of Toc159 out of the soluble cell extract. (A) Leaf extract was prepared according to the materials and methods. The pellet (lanes 1-3) or supernatant (lanes 4, 5) of the 500 × g (lane 1), 100,000 × g (lanes 2, 4) and 300,000 × g (lanes 3, 5) centrifugation step were loaded in equivalent amounts onto the chloroplast pellet on SDS-PAGE and immunodecorated with indicated antibodies. (B) The lipid content of the supernatant fractions (see (A)) was analysed by separation over TLC plate. Standard lipids were applied: sulphochinovosyldiglyceride (SL), phosphatidylinositol (PI), phosphatidylglyceride (PG), monogalactosyldiacylglyceride (MGDG), digalactosyldiacylglyceride (DGDG) and phosphatidylcholine (PC).

are truly soluble forms or a result of partly disrupted chloroplasts leading to low-density membrane shreds. Initially the lipid content of the supernatants was analysed. MGDG and DGDG were present in both supernatant fractions (Fig. 3.10 B, lane 4, 6). The synthesis and presence of galactolipids within the plant cell is restricted to chloroplasts [47] indicating the existence of

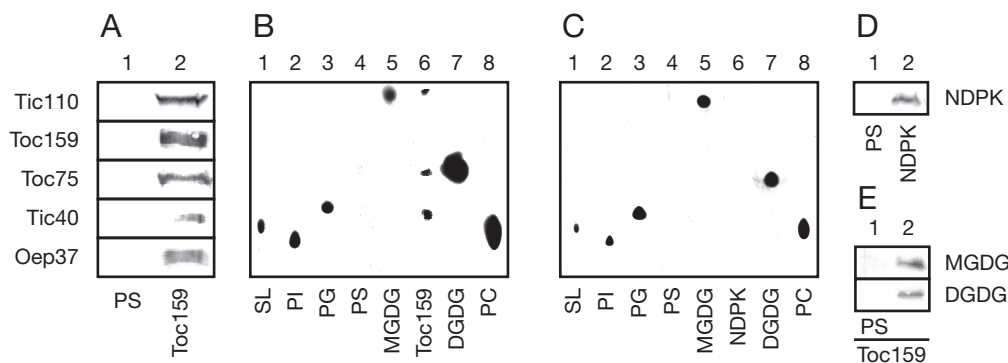


Figure 3.11: Coimmunoprecipitation. The 100,000 × g supernatant was used for coimmunoprecipitation with Toc159 (A, lane 2), NDPK (D, lane 2), MGDG (E up, lane 2) or DGDG-antiserum (E down, lane 2) and their corresponding preimmunsera (A, D, E lane 1). The precipitate was analysed for the presence of chloroplast envelope proteins (A) or Toc159 (E) by immunostaining and lipids were analyzed by extraction (B, C).

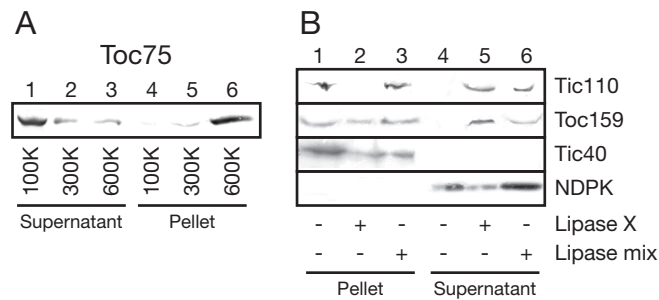


Figure 3.12: Liposome control. (A) Proteoliposomes containing Toc75 were centrifuged at $100,000 \times g$, $300,000 \times g$ and $600,000 \times g$. Supernatants (lanes 1-3) and pellets (lanes 4-6) were immunodecorated with Toc75 antiserum. (B) The soluble extract from $100,000 \times g$ centrifugation (see Fig. 3.10 A) was incubated in the absence (lanes 1, 4) or presence of lipase X (lanes 2, 5) or lipase mixture (lanes 3, 6) and subsequently subjected to a $600,000 \times g$ centrifugation. Pellets (lanes 1-3) and supernatants (lanes 4-6) were immunodecorated with the appropriate antibodies.

chloroplast membrane shreds. Next, the question of presence of a ‘soluble’ form of Toc159 in membrane shreds was addressed by using Toc159 antiserum for coimmunoprecipitation. Translocon components as well as Oep37 were coimmunoprecipitated by Toc159 antiserum (Fig. 3.11 A, lane 2). Moreover, chloroplast lipids like MGDG and DGDG were also identified in the precipitate (Fig. 3.11 B, lane 6). In contrast, neither chloroplast envelope proteins nor lipids were precipitated by preimmuneserum (Fig. 3.11 A, lane 1; Fig. 3.11 B, lane 4). When the soluble nucleoside diphosphate kinase (NDPK) was immunoprecipitated (Fig 3.11 D, lane 2), neither lipids (Fig. 3.11 C, lane 6) nor other proteins (not shown) could be detected. To confirm the lipid association of Toc159 antibodies against MGDG or DGDG were used [82]. Toc159 was successfully precipitated by these antibodies (Fig. 3.11 E, lane 2), confirming its lipid association.

To confirm these results it was important to demonstrate that membrane fragments with low protein content can not be pelleted under the described conditions [37]. For that proteoliposomes containing Toc75 were centrifuged ($100,000 \times g$ or $300,000 \times g$, 2 h). Indeed, Toc75 proteoliposomes remained in the supernatant (Fig. 3.12 A, lane 1, 2). Only after centrifugation at $600,000 \times g$ for 2 h Toc75 proteoliposomes were recovered in the pellet fraction (Fig. 3.12 A, lane 6). Therefore, it was investigated if Toc159 can be pelleted out of the leaf extract at $600,000 \times g$. After centrifugation for 2 h Toc159 could only be detected in the pellet together with Tic110 and Tic40 (Fig. 3.12 B, lane 1, 4). In contrast, the soluble nucleoside diphosphate kinase (NDPK) remained in the supernatant (lane 6). Additional evidence that the $600,000 \times g$ pelleted envelope proteins are embedded in membrane fragments was obtained by treating the cell extract with phospholipases to disrupt bilayer structure and integrity. After phospholipase treatment some of the Toc159 and Tic110 appeared in the supernatant of the $600,000 \times g$ spin

Table 3.4: Gene expression and protein ratio of the components of the plastid preprotein translocon. Given are the normalized values of transcript levels according to signal intensity by Affymetrix analysis (transcript level) and protein molarity (protein level). Values represent at least three independent measurements, and standard deviation for almost all values (IE/OE) was below 20%. Abbreviations found in the table: n.h., no homologue in *A. thaliana*; n.p., no expressed or pure protein at present; n.d., not determined.

Protein	Transcript level		Protein level		
	Leaves	Roots	OE	IE	
Toc159	1.37	0.69	0.13		
Toc132	0.40	0.80			
Toc120	0.01	0.27			
Toc190	0.19	0.16			
Toc33	0.79	0.33	0.17		
Toc34	0.35	0.63			
Toc64-I	0.24	0.24	0.07		
Toc64-III	0.20	0.13			
Toc75-V	0.27	0.24	n.p.		
Toc75-III	1.00	1.00	1.00		
Toc12	n.h.	n.d.	0.01		
Tic110	1.00	1.00			1.00
Tic62	0.74	0.10			0.11
Tic55	1.46	0.14		n.p.	
Tic40	0.71	0.55		0.96	
Tic32	0.41	0.47		0.77	
Tic22	0.50	0.53	0.002	0.02	
Tic22'	0.32	0.36			
Tic20-I	0.16	0.30		0.14	
Tic20-IV	0.02	0.34			

(Fig. 3.12 B, lane 5, 6). Only Tic40 remained in the pellet (lane 2, 3), which might be caused by aggregation. Again, the NDPK distribution was not affected by the addition of lipases (lane 5, 6).

3.4 Translocon subunits in green and non-green tissues

3.4.1 Gene expression of the Toc components

Photosynthetic and non-photosynthetic proteins were proposed to use different Toc33 and Toc159 isoforms [60]. Therefore, the possibility of differential gene expression of Toc isoforms in pho-

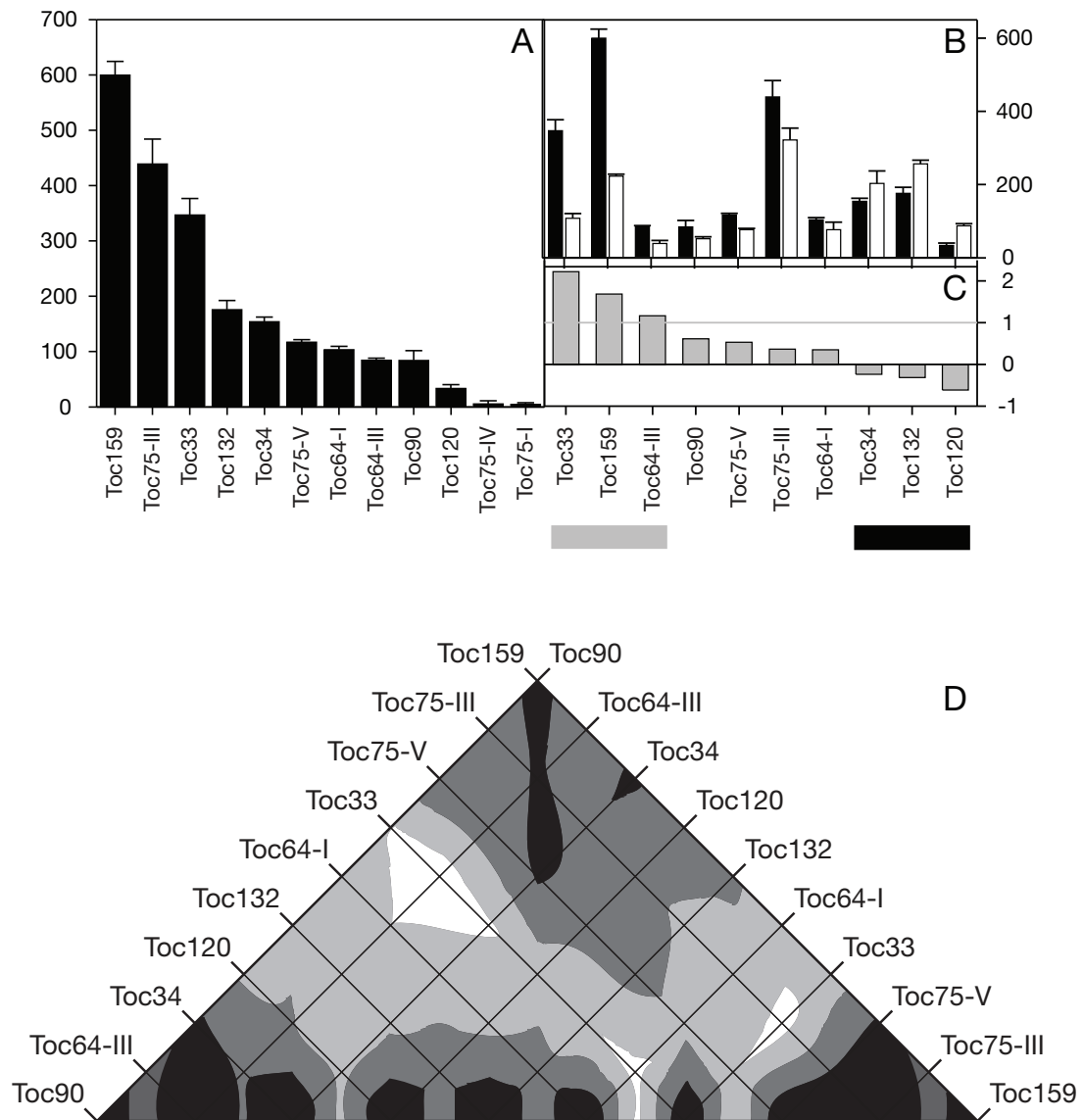


Figure 3.13: Gene expression of Toc components. (A) Gene expression of the Toc components in leaves as determined by Affymetrix expression analysis. Normalized signal intensities are shown as expression. (B) Expression levels of the Toc components in roots (white) and leaves (black). In (C) The ratio between leaf and root expression is given. Proteins with pronounced expression in leaves or roots are highlighted in gray and black, respectively. In (D), the correlation of the diurnal expression of Toc components in whole plants is shown. Dark areas correspond to small changes in the diurnal expression level, and bright areas correspond to drastic differences in the diurnal expression.

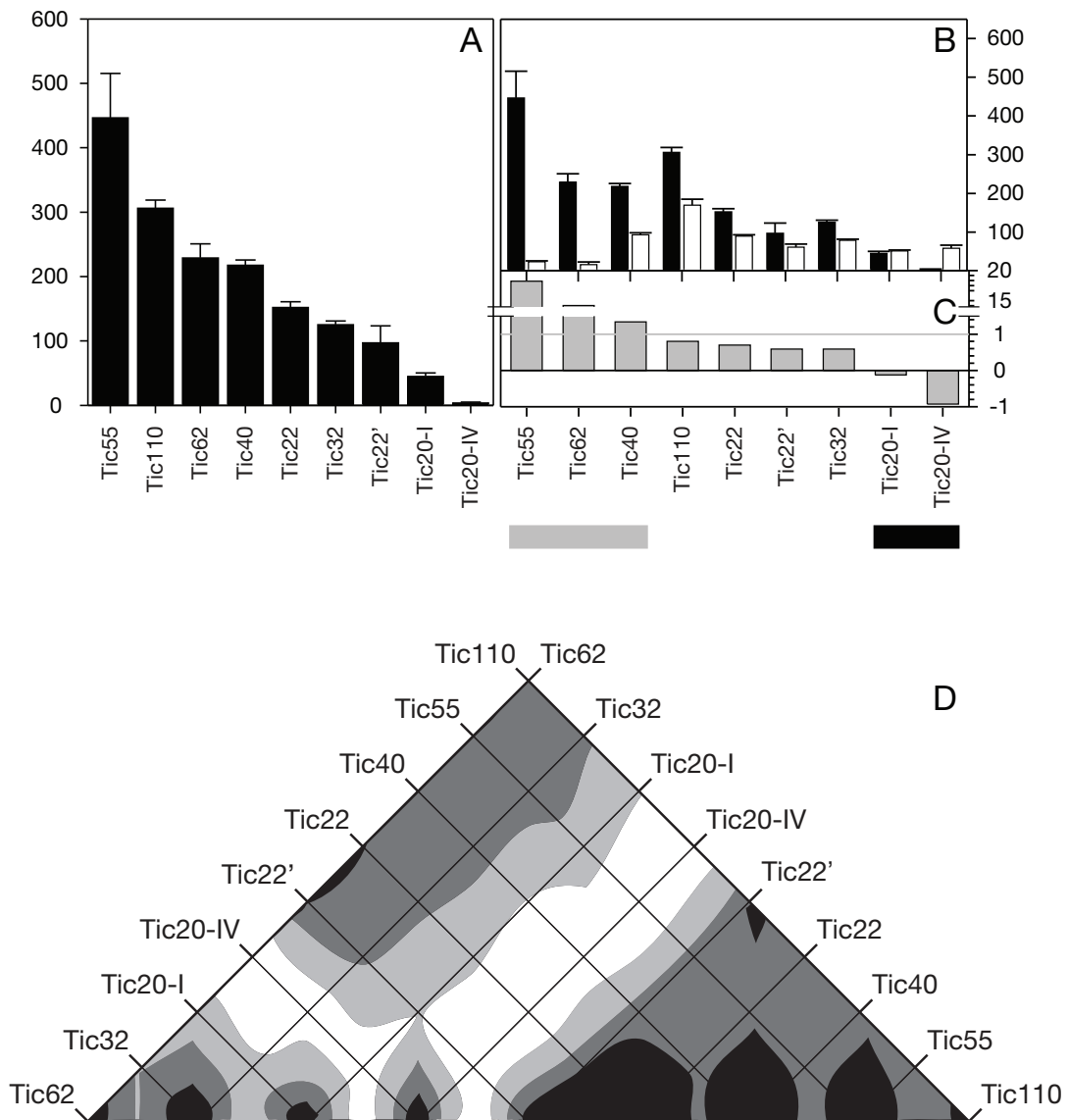


Figure 3.14: Gene expression of Tic components. A and B, gene expression of Tic components in leaves (A) and roots (B). C and D, the comparison between both (C) and diurnal changes (D) as described in the legend for Fig. 3.13 for the Toc proteins.

Table 3.5: Protein ratio in chloroplasts and amyloplasts. Amyloplasts were isolated from pea roots grown in a hydroponic culture essentially as described in [112]. The molar ratio was normalised to Toc75.

Protein	Amyloplasts	chloroplasts
Toc75	1.00	1.00
Toc64	0.57	0.10
Toc34	0.08	0.13
Tic40	0.12	0.24
Tic32	0.11	0.19

tosynthetically active and inactive tissues was investigated by gene chip analysis. The data show the highest expression levels for Toc159, Toc75-III and Toc33 (Table 3.4, Fig. 3.13 A). These proteins form the core complex for translocation across the outer envelope [90]. Interestingly, Toc132, Toc 90, Toc34, Toc75-V and the two isoforms of Toc64 showed similar expression, which is lower than the expression of Toc75-III. Only Toc120 was further reduced and no expression of Toc75-I and Toc75-IV could be detected.

In roots all the analysed genes were expressed with the exception of Toc75-IV and Toc75-I. A comparison of expression shows higher transcript levels of receptors Toc33, Toc159 and Toc64-III in leaves than in roots (Fig. 3.13 B, C). This is in line with the pale or white phenotype of Toc33 or Toc159 knock out mutants [60, 6]. Three proteins showed significantly higher expression in roots than in leaves, namely Toc34, Toc132 and Toc120. None of these three isoforms was able to complement the knockout either completely (in case of Toc33, [34, 60]) or at all (in case of Toc159, [6]) their respective isoform in leaves. The ratio of expression of Toc75 isoforms is similar in leaves and roots. Assuming that both isoforms are involved in preprotein translocation suggests that the specification of the complexes for photosynthetic and non-photosynthetic proteins is defined by receptor components and not by the channel protein.

A similar conclusion can be drawn from analysis of the diurnal gene expression (Fig. 3.13 D). Gene expression of Toc75-III and Toc75-V do not differ drastically (dark area). The same was observed for Toc90/Toc159 and Toc120/Toc132 receptor pairs but not for other combinations of these receptors. Toc33 and Toc34 also differ drastically in their expression (white area). Again, the results point to dynamic Toc composition for differential preprotein recognition.

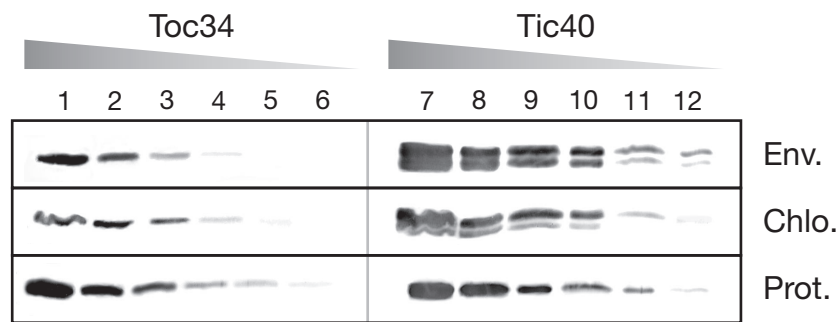


Figure 3.15: Analysis of protein amounts. The analysis for quantification of an outer (Toc34, lanes 1-6) or inner envelope protein (Tic40, lanes 7-12) is shown as an example. In total, 0.3, 0.1, 0.03, 0.01, 0.003, or 0.001 μg of protein (Prot., lanes 1-6 or 7-12), chloroplasts of 17, 5.1, 1.7, 0.51, 0.17, or 0.051 μg of chlorophyll (Chlo., lanes 1-6 or 7-12), 11.6, 3.48, 1.16, 0.35, 0.12, or 0.035 μg of purified inner envelope (Env., lanes 7-12), or 7.18, 2.16, 0.72, 0.22, 0.072, or 0.022 μg of purified outer envelope (Env., lanes 1-6) were separated on SDS-PAGE followed by immunodecoration with indicated antibodies.

3.4.2 Gene expression of the Tic components

Analysing the gene expression of the Tic components in leaves revealed that Tic55 and Tic110 are the most abundant transcripts (Table 3.4, Fig. 3.14). Only the Tic20-IV transcript could not be detected in leaves (Fig. 3.14 A) but was found in roots (Fig. 3.14 B). Tic55 is almost exclusively expressed in green tissue (Fig. 3.14 B, C). Tic40 is also predominantly expressed in green tissues. All other analysed Tics are expressed almost similarly in leaves and in roots, with the exception of Tic20-IV. Diurnal expression patterns of the Tic proteins did not fluctuate with the exception of the two Tic20 isoforms (Fig. 3.14 D).

3.4.3 Protein level of the Toc and Tic components

Differential expression levels might also reflect differential stability of the analysed proteins and might not directly correlate to protein content. Therefore, the protein concentration of the known Toc and Tic subunits in isolated envelope membranes of pea (*Pisum sativum*) was analysed (Fig. 3.15, lane 1–3). For some of the subunits the amount was also analysed in amyloplasts (Table 3.5) and chloroplasts (lane 4–9). Serial dilutions of expressed proteins were used for quantitation (lane 10–12).

Gene expression of Toc159 and Toc34, normalised to the expression level of Toc75-III is 4–6 times higher than the protein content in relation to Toc75 (Table 3.4). This could indicate decreased stability of the receptor proteins. Toc64, Toc12 and isHsp70 are less abundant than

the other components. In addition to these three low abundant proteins Tic22 could be detected in quantitative amounts in the outer envelope. This result points to a subcomplex architecture involving all four components.

For most of the Tic components no significant alteration of the protein content profile in comparison to the gene expression profile could be observed. The only proteins drastically differing were Tic22 and Tic62. Tic22 was formerly described as a soluble IMS protein and here only the membrane associated protein and not the total protein content was quantified. In line with this observation small amounts of the proteins were detected in the outer envelope.

Analysing chloroplasts, a similar protein ratio between the Toc components as in the OE was observed (Table 3.5). Furthermore, calculating the ratio between the amount of Tic components found in chloroplasts (Table 3.5) and found in the IE (Table 3.4) reveals a protein ratio between Toc75 and Tic110 of 1.4, which agrees with the estimation from the envelope protein content.

The analysis of the protein level (Fig. 3.15) in amyloplasts revealed a higher protein level of Toc64 than Toc34. However, gene expression of the two isoforms of Toc34 in *A. thaliana* (Table 3.4) revealed a higher expression of the gene atToc33, the homologue of Toc34 in *Pisum sativum* [45] in leaves in comparison to the gene expression of atToc34. The opposite is true for the root plastids: the dominant isoform is in this case atToc34. Since the second isoform in *P. sativum* has not been identified so far, cross reactivity of the used antibodies with the second isoform could not be confirmed. Therefore, taking into account the possibility of existence of the second Toc34 isoform in *P. sativum* and the probable cross-reactivity of the antibody against it, the result might reflect that psToc34 is less abundant in amyloplasts, which would be in line with the gene expression analysis. The protein ratio found for the Tic components investigated (Table 3.5) is similar to the corresponding gene expression ratio.

Chapter 4

Discussion

4.1 Toc complex reconstitution

4.1.1 A new technique for liposome size determination

Partial solubilization is often used for reconstitution of proteins into liposomes [3]. Therefore, it has been demonstrated that the concentration required to reach the transition state where liposomes start to solubilize depends on the liposome number in the case of dodecylmaltoside and on the lipid concentration in the case of octylglucoside. For practical use, the concentration (in the case of solubilization by octylglucoside) and the size and lipid concentration (in the case of solubilization by dodecylmaltoside) must be known. Therefore, a system for size determination by absorption spectroscopy was established (see 3.1.4) because the instruments required for DLS are not available in a typical molecular biology/biochemistry laboratory. To this end, a technically simple method requiring only ubiquitous laboratory instrumentation (a spectrophotometer) has been developed. It enables determination of liposome size and/or lipid concentration in a single spectrophotometric measurement. Once the calibration plots are prepared and the curve parameters are determined, results of one or (better) two measurements can be translated into liposome size and concentration directly by numerical means. This method is quick and simple when compared to DLS, the current standard for liposome size determination.

4.1.2 Purification and reconstitution of the Toc complex

Reconstitution into proteoliposomes is used in study of many membrane proteins [106, 87, 116], and represents a valuable tool in research of the Toc complex. Working protocols for Toc complex isolation and reconstitution already exist [90], but their use on a large scale requires further

optimization aimed at a higher efficiency. This is a problem not unique to the import field [115]. Techniques for purification and reconstitution of the Toc complex are in essence similar to those used by other researchers of membrane proteins [42], and suffer the same problems—namely a low yield of standard purification procedures.

Successful purification protocols in the field of protein translocation, for instance the SecYEG component of the bacterial Sec translocase [106, 107] and the Tom core [1] as well as the soluble Tim9/Tim10 [108] complex of mitochondria rely on the (over)expression of labeled proteins, which makes the isolation a simple matter. Particularly interesting is the isolation of the Tom core complex [1] where only one component (Tom22) is exchanged with its artificial hexahistidine tagged version in the fungus *Neurospora crassa*, which facilitates the subsequent purification of the solubilized complex. However, it should be noted that such manipulations are much more easily performed on readily transformable haploid organisms such as *E. coli* and *N. crassa* than on plants, even in the case of the model organism *A. thaliana*. For Toc complex purification, either the existing protocol [90] should be optimized further, or a completely new approach has to be developed. In every case, chloroplasts are to be preferred over the isolated outer envelope as the starting material for purification of the Toc complex, since they are readily obtained and their use alleviates the problem of complex disruption and inactivation during isolation.

Reconstitution of the Toc complex has been attempted using a protocol similar to one of several that were successful with the SecYEG complex [87]. It is based on gradual detergent removal using detergent adsorbing properties of polystyrene beads [85, 84]. When larger amounts of the isolated material are available, other reconstitution approaches, such as methods involving giant unilamellar vesicles [33] or rapid detergent dilution [14, 106] can be attempted.

4.2 Toc159 is a membrane inserted protein

Toc159 was first described as an integral membrane protein [49]. However, the hypothesis that it acts as a soluble receptor was formed based on Toc159 being found in the cytosol after cell fractionation [37]. The idea could be further advocated by drawing a parallel with the ATPase driven SecA-type protein translocation [65] where the initial soluble receptor sequesters its target and transports it to the rest of the translocation machinery. However, there is no solid evidence for such a mechanism in chloroplasts, since it has been demonstrated that the identified soluble Toc159 indeed represents a membrane bound population present in lipids shreds, which do not pellet by a simple $100,000 \times g$ centrifugation step. Toc159 presence in the cytosol was therefore shown to be an artifact introduced during isolation [9]. Furthermore, although the Toc159 itself

has affinity for the transit sequence, Toc34 seems to be the primary precursor protein receptor, with the polypeptide being handed over to the Toc159 from the initial receptor Toc34 in a later step [9]. Moreover, Toc159 is unlikely to be a cytosolic protein since the 52 kDa M-domain comprises an intermembrane space facing part, which might contain multiple membrane spanning regions, and can not be extracted from the membrane [7]. Evidence for the membrane bound Toc159 can therefore be considered satisfactory, and even the original proponents of the soluble receptor hypothesis seem to have stopped mentioning it in their recent work on chloroplast import [51].

Taking into account the localization of Toc159, it follows that all interactions between precursor proteins, Toc159 and Toc34 must occur on the membrane. The initial receptor Toc34 has higher affinity for phosphorylated presequence of precursor proteins than Toc159, and the handover is facilitated by the GTP hydrolysis cycle of Toc34 and dephosphorylation of the presequence [45, 9]. This has profound consequences for the model of action of Toc159. A soluble receptor would have been just a means of delivery and targeting, the latter function being redundant with that of the guidance complex. In contrast, a membrane bound secondary receptor can be envisaged as a molecular motor driving the first steps of translocation, especially when its stoichiometry in the complex [90] and its GTPase activity which could energize the power stroke [56] are taken into account.

4.3 Toc complexes with different subunit compositions

4.3.1 Expression in green and non-green tissues

Comparing the expression of the Toc and Tic components revealed a 1.43-fold higher expression rate of Toc75-III in comparison to Tic110 in leaves, and a 1.90-fold higher expression rate in roots. This might be explained as follows: the OE translocon has to translocate proteins targeted to the IE and to the stroma. Different routes may exist for these two compartments. However, due to the existence of the thylakoid system, which contains the photosynthetically active proteins in chloroplasts, a higher translocation rate across the IE is required in comparison to amyloplasts, which do not contain thylakoids. This would lead to an increased Tic/Toc ratio in chloroplasts compared to non-green plastids.

4.3.2 Expression of different subunits

Differential expression levels might also reflect differential stability of the proteins and might not directly correlate to the protein content. Therefore, the protein concentration of the known Toc and Tic subunits in isolated envelope membranes was analysed. For some of the subunits the amount was also analysed in amyloplasts and chloroplasts.

The relatively high transcript content of receptors Toc34 and Toc159 in comparison with Toc75 indicates decreased stability of the receptor proteins. This points to a high turnover which might have a physiological role as a means of regulation of these subunits. Toc64, Toc12 and isHsp70 were found to be relatively less abundant. In addition to these three low abundant proteins Tic22 could be detected in quantitative amounts in the outer envelope. This result points to a subcomplex architecture. Such a complex involving all four components can be isolated (Schleiff, unpublished). The low abundance of these proteins might indicate a specialised function. Taking the proposal of Kouranov et al. [57], this complex might translocate preproteins which are then further translocated by the Tic20 pathway.

The large discrepancy between gene expression and protein levels of Toc34 and Toc159 leads to the question, whether these two proteins are less stable than the protein channel. Since both proteins face the cytosol and are phosphorylated it might be that this event is involved in signaling for degradation. It could also be thought that both receptors are partly soluble and therefore not detectable in the membranes. However, this contradicts the current knowledge, especially on Toc34.

The only Tic components with a different expression profile compared to protein content were Tic22 and Tic62. Tic22 could not be conclusively quantified since it is an IMS protein found associated with both the inner and, to a lesser extent, outer envelope. Tic62 is involved in redox regulation of protein translocation [62]. The reduced ratio of Toc62 compared to Tic110 might therefore represent a high turnover.

From the protein ratio and from the gene expression data it can be excluded that Tic20 forms the channel for stromal-targeted proteins [57] since a 10 fold molar excess of Toc75 over Tic20 is present in chloroplasts. However, Tic20 might be involved in a translocation pathway of other proteins. A system similar to the one operating in mitochondrial inner membrane can be envisaged in chloroplasts. In this case, Tic110 would be analogous to the Tim17/Tim23 import channel for mitochondrial matrix proteins, while Tic20 could represent an important component of another import system, perhaps similar to Tim22 complex which imports proteins destined for the inner mitochondrial membrane [104, 95].

For the two channel-forming proteins we observed 1.3 pmol Tic110 per μg IE and 5.4 pmol

Toc75 per μg OE of chloroplasts (Table 3.4). Taking into account that protein density in the IE is three times higher than in the OE [10] a ratio between Toc75 and Tic110 of 1.4 in chloroplasts can be calculated. This correlates well with the transcript ratio. The ratio between Toc75 and Tic110 in chloroplast envelope membranes might be explained by a pore structure composed of two or three Tic110 proteins or a second pathway requiring the action of Toc75 or Tic110 individually. The ratio between Toc75 and Tic110 of 1.4 in chloroplast envelopes also reveals information about the relation of total protein content in envelope membranes, and agrees with previous results [23].

From the expression analysis it can be speculated that two distinct receptor complexes exist (Fig. 4.1). The first complex would be more specific for photosynthetic proteins, predominantly expressed in green tissues and composed of Toc159, Toc90 and Toc33. This would explain their existence in leaves (Fig. 3.13) and the observed phenotypes in *ppi1* and *ppi2* mutants [60, 6]. The low expression level of Toc90 however, is consistent with the *ppi2* phenotype. The second complex would be more specific for the housekeeping proteins and composed of Toc132, Toc120 and Toc34, explaining why both complexes coexist in the same tissues (Fig. 3.13). Further support for the existence of two complexes comes from the presequence preference of the two *Arabidopsis* Toc34 isoforms. While atToc33 is highly expressed in leaves and shows strong stimulation of its GTPase activity by photosynthesis-specific precursor proteins, atToc34 is located primarily in roots and strongly activated by nonphotosynthetic precursor proteins [34, 45].

4.4 The current model of protein translocation into chloroplasts

Localization of Toc159 in the membrane and its four times lower abundance in the complex when compared to Toc34 are in line with the Toc complex structure suggested by [90], where Toc159 is placed in the center of the complex and surrounded by four of each Toc75 and Toc34 subunits. Such configuration, especially in the context of other research on preprotein recognition [9], supports the notion that Toc34 acts as the primary receptor. Therefore, binding of preproteins takes place on the chloroplast outer envelope. In contrast to the so-called targeting hypothesis [51], where Toc159 acts as the primary receptor and together with Toc34 commits the preprotein to the import pore, current model ascribes a motor function to Toc159—after taking over a preprotein from Toc34, it actively carries out the first steps of import by undergoing a conformational change and pushing the N-terminus of the preprotein through one of the four Toc75 pores. Since import depends on GTP being available on the cytosolic side of the envelope, and Toc159 and

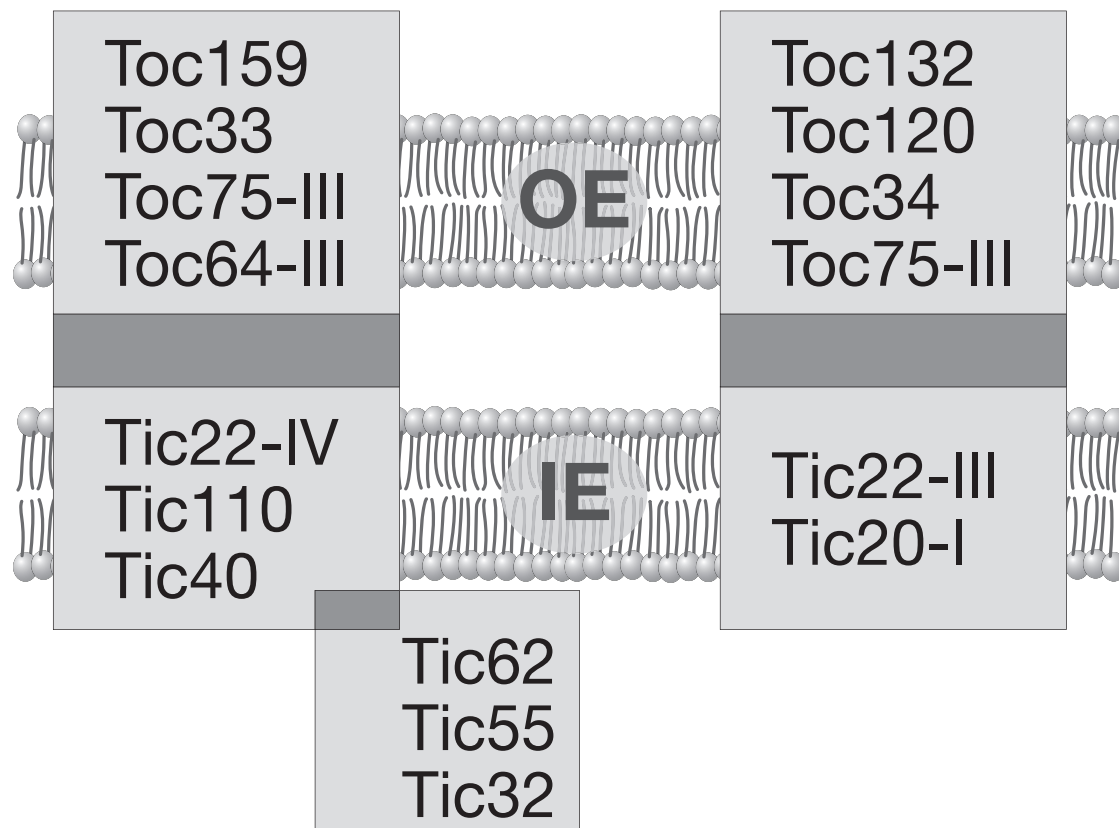


Figure 4.1: Different Toc complexes with distinct functions in *Arabidopsis thaliana*. Based on the expression in photosynthetic (leaves) and nonphotosynthetic (roots) tissues, two dominant subunit compositions can be identified, each corresponding to a different type of the Toc complex. Both types are built around the atToc75-III pore. The type preferentially used for photosynthetic proteins (left) uses atToc159 and atToc33 isoforms of GTPase receptors. AtToc64-III seems to be associated with this type as well. The other type (right) imports mostly ‘housekeeping’ proteins, i.e. plastid proteins not directly involved in photosynthesis. It consists of atToc132, atToc120 and atToc34, in addition to Toc75-III. Association with Toc64 doesn’t seem to play a significant role in this type of the complex. Interestingly, different Tic isoforms seem to be coexpressed with the two Toc complex types.

Toc75 alone are able to carry out protein import into artificial liposomes [90], GTPase activity of Toc159 can be seen as providing energy for initial steps of protein import into chloroplasts.

The G-domain of GTPases carries out nucleotide binding and hydrolysis. This ~20 kDa domain consists of a mixed six-stranded β sheet and five helices located on both sides [109, 101]. The structural units are organized into three motifs: the switch I, switch II and the P-loop regions, connected to nearby β -strands. The catalytic domain functions as a conformational switch, with significant structural differences between the strained GTP bound and the relaxed GDP bound

state. Catalytic domains of G proteins and those of ATP-hydrolysing motor proteins share a degree of similarity in structure and mechanism of action, with a power stroke in the range of 10 pN in both cases [56]. Unlike ATP dependent motor proteins, the known G proteins lack a ‘lever arm’ to produce large-amplitude displacements. This mechanism can be envisaged as the driving force behind the conformational change which facilitates preprotein translocation by Toc159.

In contrast to the mitochondrial ‘acid chain’ hypothesis [86, 55], transfer across the outer envelope itself remains energy dependent. Toc159 actively pushes the precursor protein through the translocation pore, enough to expose a string of amino acid residues to the other side [88]. Subsequently, there has to be a mechanism which could provide enough energy to power the complete import reaction *in vivo*. Likely candidates for this mission are molecular chaperones, abundant in both the stroma and the intermembrane space of chloroplasts. The idea is not new—more than a decade ago, researchers envisaged a system similar to a Brownian ratchet which could drive protein import into organelles [94, 70]. Subsequently an alternative so-called power stroke model was proposed [70]. Both models were extensively theoretically investigated in order to confirm the validity of one or the other based on the kinetic data [27]. The more than a decade long debate seems to be settled by reconciliation of the two models proposing a mechanism called entropic pulling [25]. According to the entropic pulling model, thermal fluctuations are rectified by a free-energy gradient, without a requirement for an anchor or even a pore. This single mechanism is able to explain different functions of Hsp70, functional differences depending on co-chaperones (such as J domain), nucleotide exchange factors or docking. Also, in this model chaperones do not need a molecular fulcrum and the energy produced is sufficient to explain quick import, even of proteins that require partial unfolding. Hence, *in vivo* final translocation after initial push by Toc159 might be assisted by IMS localized Hsp70 [66, 113, 93].

Chapter 5

Conclusion

The aim of this study was the analysis of the Toc complex composition, function and dynamics. To this end, several questions have been addressed.

First, the composition of the functional Toc core complex was investigated. Analyses of the complex stoichiometry have provided support for the ‘classical’ Toc core complex consisting of Toc75, Toc34 and Toc159, with dynamically associated Toc64, which is itself a member of another intermembrane space complex. Different subunit isoforms seem to assemble different Toc complexes with different preprotein preference—the complex consisting of atToc159, atToc33, atToc75-III and atToc64-III more specific for photosynthetic proteins and strongly expressed in green tissues, and the complex made of atToc132/atToc120, atToc34 and atToc75-III representing the pathway to chloroplasts for nonphotosynthetic ‘housekeeping’ proteins expressed to a higher level in nonphotosynthetic tissues. Lower abundance of Toc64, Toc12, isHsp70 and Tic22 points to their arrangement in a subcomplex, which might be involved in import of proteins further translocated by the Tic20 pathway.

Second, the localization of Toc159 was re-investigated. The protein was found to be firmly embedded in the membrane. Hence, the proposal of cytosolic action of a soluble form of Toc159 had to be rejected based on the obtained results. Placing the Toc159 in the membrane helps to settle another, perhaps even more important question: which receptor acts first, Toc34 or Toc159? Toc159 is four times less abundant in the envelope than Toc34 which favors a membrane inserted Toc159 as the central component of the complex. The action of Toc159 has therefore to be seen as occurring after the initial recognition step, which is most likely carried out by Toc34.

For further analysis of the Toc translocon structure and the mode of its action, it was necessary to develop tools which would facilitate study of the Toc complex in a particularly well suited model system, the proteoliposomes. To this end, a method has been developed to deter-

mine liposome size and concentration in a single spectrophotometric measurement. Attempts to develop an efficient Toc complex isolation and reconstitution protocol were not successful, but the research done in the pursuit of this goal provides solid foundations for future efforts.

Appendix A

Abbreviations

ADP	adenosine diphosphate	Mw	molecular weight
ATP	adenosine triphosphate	NAD(P) ⁺	nicotinamide adenine dinucleotide (phosphate), oxidized form
A _{xxx}	absorbance at the wavelength of xxx nm	NDPK	nucleoside diphosphate kinase
CMC	critical micelle concentration	OD	optical density
DeMa	decyl-β-D-maltoside	OE	outer envelope
DGDG	digalactosyldiacylglycerol	OE-LM	outer envelope lipid mixture
DLS	dynamic light scattering	OG	n-octyl-β-D-glucoside
DoMa	dodecyl-β-D-maltoside	PAGE	polyacrylamide gel electrophoresis
EM	electron microscopy	PC	phosphatidylcholine
GDP	guanosine diphosphate	PCR	polymerase chain reaction
GTP	guanosine triphosphate	PG	phosphatidylglycerol
Hsp	heat shock protein	PI	phosphatidylinositol
IE	inner envelope	pSSU	precursor of the small subunit of RuBisCO
IE-LM	inner envelope lipid mixture	RuBisCO	ribulose-1,5-bisphosphate carboxylase/oxygenase
IMS	intermembrane space	SDS	sodium dodecyl sulfate
IP	immunoprecipitation	SL	sulfolipid (Sulfoquinovosyldiacylglycerol)
IPTG	isopropyl-β-D-thiogalactopyranoside	Tic	translocon on the inner envelope of chloroplasts
isHsp	intermembrane space heat shock protein	Toc	translocon on the outer envelope of chloroplasts
LHCPII	light-harvesting chlorophyll binding protein of photosystem II	TPR	tetratrico peptide repeat
MGDG	monogalactosyldiacylglycerol		

Bibliography

- [1] U. Ahting, C. Thun, R. Hegerl, D. Typke, F. E. Nargang, W. Neupert, and S. Nussberger. The TOM core complex: the general protein import pore of the outer membrane of mitochondria. *J. Cell Biol.*, 147:959–68, 1999.
- [2] M. Akita, E. Nielsen, and K. Keegstra. Identification of protein transport complexes in the chloroplastic envelope membranes via chemical cross-linking. *J. Cell Biol.*, 136:983–94, 1997.
- [3] M. Angrand, A. Briolay, F. Ronzon, and B. Roux. Detergent-mediated reconstitution of a glycosyl-phosphatidylinositol-protein into liposomes. *Eur. J. Biochem.*, 250:168–76, 1997.
- [4] D. J. Arnon. Copper enzymes in isolated chloroplasts. Polyphenoloxidase in *Beta vulgaris*. *Plant Physiol.*, 24:42–45, 1949.
- [5] A. Baldwin, A. Wardle, R. Patel, P. Dudley, S. K. Park, D. Twell, K. Inoue, and P. Jarvis. A molecular-genetic study of the *Arabidopsis* Toc75 gene family. *Plant Physiol.*, 138:715–33, 2005.
- [6] J. Bauer, K. Chen, A. Hiltbunner, E. Wehrli, M. Eugster, D. Schnell, and F. Kessler. The major protein import receptor of plastids is essential for chloroplast biogenesis. *Nature*, 403:203–7, 2000.
- [7] J. Bauer, A. Hiltbrunner, P. Weibel, P. A. Vidi, M. Alvarez-Huerta, M. D. Smith, D. J. Schnell, and F. Kessler. Essential role of the G-domain in targeting of the protein import receptor atToc159 to the chloroplast outer membrane. *J. Cell Biol.*, 159:845–54, 2002.
- [8] T. Becker, J. Hritz, M. Vogel, A. Caliebe, B. Bukau, J. Soll, and E. Schleiff. Toc12, a novel subunit of the intermembrane space preprotein translocon of chloroplasts. *Mol. Biol. Cell*, 15:5130–44, 2004.
- [9] T. Becker, M. Jelic, A. Vojta, A. Radunz, J. Soll, and E. Schleiff. Preprotein recognition by the Toc complex. *EMBO J.*, 23:520–30, 2004.
- [10] M. A. Block, A. J. Dorne, J. Joyard, and R. Douce. Preparation and characterization of membrane fractions enriched in outer and inner envelope membranes from spinach chloroplasts. II. Biochemical characterization. *J. Biol. Chem.*, 258:13281–6, 1983.

- [11] M. Bogdanov and W. Dowhan. Phospholipid-assisted protein folding: phosphatidylethanolamine is required at a late step of the conformational maturation of the polytopic membrane protein lactose permease. *EMBO J.*, 17:5255–64, 1998.
- [12] B. D. Bruce. The role of lipids in plastid protein transport. *Plant Mol. Biol.*, 38:223–46, 1998.
- [13] B. D. Bruce. The paradox of plastid transit peptides: conservation of function despite divergence in primary structure. *Biochim. Biophys. Acta*, 1541:2–21, 2001.
- [14] L. Brundage, J. P. Hendrick, E. Schiebel, A. J. Driessen, and W. Wickner. The purified *E. coli* integral membrane protein SecY/E is sufficient for reconstitution of SecA-dependent precursor protein translocation. *Cell*, 62:649–57, 1990.
- [15] N. J. Butterfield. *Bangiomorpha pubescens* n. gen., n. sp.: implications for the evolution of sex, multicellularity, and the mesoproterozoic/neoproterozoic radiation of eukaryotes. *Paleobiology*, 26:386–404, 2000.
- [16] A. Caliebe, R. Grimm, G. Kaiser, J. Lübeck, J. Soll, and L. Heins. The chloroplastic protein import machinery contains a Rieske-type iron-sulfur cluster and a mononuclear iron-binding protein. *EMBO J.*, 16:7342–50, 1997.
- [17] K. Chen, X. Chen, and D. J. Schnell. Initial binding of preproteins involving the Toc159 receptor can be bypassed during protein import into chloroplasts. *Plant Physiol.*, 122:813–22, 2000.
- [18] X. Chen, M. D. Smith, L. Fitzpatrick, and D. J. Schnell. *In vivo* analysis of the role of atTic20 in protein import into chloroplasts. *Plant Cell*, 14:641–54, 2002.
- [19] F. Chigri, F. Hörmann, A. Stamp, D. K. Stammers, B. Bölter, J. Soll, and U. C. Vothknecht. Calcium regulation of chloroplast protein translocation is mediated by calmodulin binding to Tic32. *Proc. Natl. Acad. Sci. USA*, in press, 2006.
- [20] F. Chigri, J. Soll, and U. C. Vothknecht. Calcium regulation of chloroplast protein import. *Plant J.*, 42:821–31, 2005.
- [21] M. L. Chou, L. M. Fitzpatrick, S. L. Tu, G. Budziszewski, S. Potter-Lewis, M. Akita, J. Z. Levin, K. Keegstra, and H. M. Li. Tic40, a membrane-anchored co-chaperone homolog in the chloroplast protein translocon. *EMBO J.*, 22:2970–80, 2003.
- [22] O. Cinquin, R. I. Christopherson, and R. I. Menz. A hybrid plasmid for expression of toxic malarial proteins in *Escherichia coli*. *Mol. Biochem. Parasitol.*, 117:245–7, 2001.
- [23] J. A. Davila-Aponte, K. Inoue, and K. Keegstra. Two chloroplastic protein translocation components, Tic110 and Toc75, are conserved in different plastid types from multiple plant species. *Plant Mol. Biol.*, 51:175–81, 2003.

- [24] E. de Leeuw, K. te Kaat, C. Moser, G. Menestrina, R. Demel, B. de Kruijff, B. Oudega, J. Luirink, and I. Sinning. Anionic phospholipids are involved in membrane association of FtsY and stimulate its GTPase activity. *EMBO J.*, 19:531–41, 2000.
- [25] P. De Los Rios, A. Ben-Zvi, O. Slutsky, A. Azem, and P. Goloubinoff. Hsp70 chaperones accelerate protein translocation and the unfolding of stable protein aggregates by entropic pulling. *Proc. Natl. Acad. Sci. USA*, 103:6166–71, 2006.
- [26] K. Eckart, L. Eichacker, K. Sohr, E. Schleiff, L. Heins, and J. Soll. A Toc75-like protein import channel is abundant in chloroplasts. *EMBO Rep.*, 3:557–62, 2002.
- [27] T. C. Elston. The brownian ratchet and power stroke models for posttranslational protein translocation into the endoplasmic reticulum. *Biophys. J.*, 82:1239–53, 2002.
- [28] F. Ertel, O. Mirus, R. Bredemeier, S. Moslavac, T. Becker, and E. Schleiff. The evolutionarily related beta-barrel polypeptide transporters from *Pisum sativum* and *Nostoc pcc7120* contain two distinct functional domains. *J. Biol. Chem.*, 280:28281–9, 2005.
- [29] U. I. Flügge. Transport in and out of plastids: does the outer envelope membrane control the flow? *Trends Plant Sci.*, 5:135–7, 2000.
- [30] H. Fulgosi and J. Soll. The chloroplast protein import receptors Toc34 and Toc159 are phosphorylated by distinct protein kinases. *J. Biol. Chem.*, 277:8934–40, 2002.
- [31] H. Fulgosi, J. Soll, S. de Faria Maraschin, H. A. Korthout, M. Wang, and C. Testerink. 14-3-3 proteins and plant development. *Plant Mol. Biol.*, 50:1019–29, 2002.
- [32] Y. Georgalis and W. Saenger. Light scattering studies on supersaturated lysozyme solution. *Cryst. Growth. Res.*, 4:1–62, 1998.
- [33] P. Girard, J. Pecreaux, G. Lenoir, P. Falson, J. L. Rigaud, and P. Bassereau. A new method for the reconstitution of membrane proteins into giant unilamellar vesicles. *Biophys. J.*, 87:419–29, 2004.
- [34] M. Gutensohn, B. Schulz, P. Nicolay, and U. I. Flügge. Functional analysis of the two *Arabidopsis* homologues of Toc34, a component of the chloroplast protein import apparatus. *Plant J.*, 23:771–83, 2000.
- [35] L. Heins, A. Mehrle, R. Hemmler, R. Wagner, M. Küchler, F. Hörmann, D. Sveshnikov, and J. Soll. The preprotein conducting channel at the inner envelope membrane of plastids. *EMBO J.*, 21:2616–25, 2002.
- [36] V. Helms. Attraction within the membrane. Forces behind transmembrane protein folding and supramolecular complex assembly. *EMBO Rep.*, 3:1133–8, 2002.
- [37] A. Hiltbrunner, J. Bauer, P. A. Vidi, S. Infanger, P. Weibel, M. Hohwy, and F. Kessler. Targeting of an abundant cytosolic form of the protein import receptor atToc159 to the outer chloroplast membrane. *J. Cell Biol.*, 154:309–16, 2001.

- [38] D. K. Hinch. Effects of calcium-induced aggregation on the physical stability of liposomes containing plant glycolipids. *Biochim. Biophys. Acta*, 1611:180–6, 2003.
- [39] D. K. Hinch, A. E. Oliver, and J. H. Crowe. The effects of chloroplast lipids on the stability of liposomes during freezing and drying. *Biochim. Biophys. Acta*, 1368:150–60, 1998.
- [40] S. C. Hinnah, K. Hill, R. Wagner, T. Schlicher, and J. Soll. Reconstitution of a chloroplast protein import channel. *EMBO J.*, 16:7351–60, 1997.
- [41] F. Hörmann, M. Kuchler, D. Sveshnikov, U. Oppermann, Y. Li, and J. Soll. Tic32, an essential component in chloroplast biogenesis. *J. Biol. Chem.*, 279:34756–62, 2004.
- [42] Y. H. Hung, M. J. Layton, I. Voskoboinik, J. F. Mercer, and J. Camakaris. Purification and membrane reconstitution of catalytically active Menkes copper transporting P-type ATPase (MNK; ATP7A). *Biochem. J.*, in press, 2006.
- [43] K. Inoue and D. Potter. The chloroplastic protein translocation channel Toc75 and its paralog OEP80 represent two distinct protein families and are targeted to the chloroplastic outer envelope by different mechanisms. *Plant J.*, 39:354–65, 2004.
- [44] P. Jarvis, L. J. Chen, H. Li, C. A. Peto, C. Fankhauser, and J. Chory. An *Arabidopsis* mutant defective in the plastid general protein import apparatus. *Science*, 282:100–3, 1998.
- [45] M. Jelic, J. Soll, and E. Schleiff. Two toc34 homologues with different properties. *Biochemistry*, 42:5906–16, 2003.
- [46] M. Jelic, N. Sveshnikova, M. Motzkus, P. Hörth, J. Soll, and E. Schleiff. The chloroplast import receptor Toc34 functions as preprotein-regulated GTPase. *Biol. Chem.*, 383:1875–83, 2002.
- [47] J. Joyard, M. A. Block, and R. Douce. Molecular aspects of plastid envelope biochemistry. *Eur. J. Biochem.*, 199:489–509, 1991.
- [48] A. A. Kelly, J. E. Froehlich, and P. Dörmann. Disruption of the two digalactosyldiacylglycerol synthase genes DGD1 and DGD2 in *Arabidopsis* reveals the existence of an additional enzyme of galactolipid synthesis. *Plant Cell*, 15:2694–706, 2003.
- [49] F. Kessler, G. Blobel, H. A. Patel, and D. J. Schnell. Identification of two GTP-binding proteins in the chloroplast protein import machinery. *Science*, 266:1035–9, 1994.
- [50] F. Kessler and D. J. Schnell. A GTPase gate for protein import into chloroplasts. *Nat. Struct. Biol.*, 9:81–3, 2002.
- [51] F. Kessler and D. J. Schnell. The function and diversity of plastid protein import pathways: a multilane GTPase highway into plastids. *Traffic*, 7:248–57, 2006.

- [52] R. V. Klassen. Modeling the effect of the atmosphere on light. *ACM T. Graphic.*, 6:215–37, 1987.
- [53] T. Kleffmann, D. Russenberger, A. von Zychlinski, W. Christopher, K. Sjölander, W. Gruissem, and S. Baginsky. The *Arabidopsis thaliana* chloroplast proteome reveals pathway abundance and novel protein functions. *Curr. Biol.*, 14:354–62, 2004.
- [54] J. Knol, K. Sjollema, and B. Poolman. Detergent-mediated reconstitution of membrane proteins. *Biochemistry*, 37:16410–15, 1998.
- [55] T. Komiya, S. Rospert, C. Koehler, R. Looser, G. Schatz, and K. Mihara. Interaction of mitochondrial targeting signals with acidic receptor domains along the protein import pathway: evidence for the ‘acid chain’ hypothesis. *EMBO J.*, 17:3886–98, 1998.
- [56] I. Kosztin, R. Bruinsma, P. O’Lague, and K. Schulten. Mechanical force generation by G proteins. *Proc. Natl. Acad. Sci. USA*, 99:3575–80, 2002.
- [57] A. Kouranov, X. Chen, B. Fuks, and D. J. Schnell. Tic20 and Tic22 are new components of the protein import apparatus at the chloroplast inner envelope membrane. *J. Cell Biol.*, 143:991–1002, 1998.
- [58] A. Kouranov and D. J. Schnell. Analysis of the interactions of preproteins with the import machinery over the course of protein import into chloroplasts. *J. Cell Biol.*, 139:1677–85, 1997.
- [59] S. Kovacheva, J. Bedard, R. Patel, P. Dudley, D. Twell, G. Rios, C. Koncz, and P. Jarvis. *In vivo* studies on the roles of Tic110, Tic40 and Hsp93 during chloroplast protein import. *Plant J.*, 41:412–28, 2005.
- [60] S. Kubis, A. Baldwin, R. Patel, A. Razzaq, P. Dupree, K. Lilley, J. Kurth, D. Leister, and P. Jarvis. The *Arabidopsis* *ppi1* mutant is specifically defective in the expression, chloroplast import, and accumulation of photosynthetic proteins. *Plant Cell*, 15:1859–71, 2003.
- [61] S. Kubis, R. Patel, J. Combe, J. Bedard, S. Kovacheva, K. Lilley, A. Biehl, D. Leister, G. Rios, C. Koncz, and P. Jarvis. Functional specialization amongst the arabidopsis Toc159 family of chloroplast protein import receptors. *Plant Cell*, 16:2059–77, 2004.
- [62] M. Kuchler, S. Decker, F. Hörmann, J. Soll, and L. Heins. Protein import into chloroplasts involves redox-regulated proteins. *EMBO J.*, 21:6136–45, 2002.
- [63] U. K. Laemmli. Cleavage of structural proteins during the assembly of the head of bacteriophage T4. *Nature*, 227:680–5, 1970.
- [64] R. C. MacDonald, R. I. MacDonald, B. P. M. Menco, K. Takeshita, N. K. Subbarao, and L.-R. Hu. Small-volume extrusion apparatus for preparation of large, unilamellar vesicles. *Biochim. Biophys. Acta*, 1061:297–303, 1991.

- [65] E. H. Manting and A. J. Driessen. *Escherichia coli* translocase: the unravelling of a molecular machine. *Mol. Microbiol.*, 37:226–38, 2000.
- [66] J. S. Marshall, A. E. DeRocher, K. Keegstra, and E. Vierling. Identification of heat shock protein hsp70 homologues in chloroplasts. *Proc. Natl. Acad. Sci. USA*, 87:374–8, 1990.
- [67] W. Martin. Gene transfer from organelles to the nucleus: frequent and in big chunks. *Proc. Natl. Acad. Sci. USA*, 100:8612–4, 2003.
- [68] T. May and J. Soll. 14-3-3 proteins form a guidance complex with chloroplast precursor proteins in plants. *Plant Cell*, 12:53–64, 2000.
- [69] T. Murashige and F. Skoog. A revised medium for rapid growth and bio assays with tobacco tissue cultures. *Physiologia Plantarum*, 15:473–97, 1962.
- [70] W. Neupert and M. Brunner. The protein import motor of mitochondria. *Nat. Rev. Mol. Cell Biol.*, 3:555–65, 2002.
- [71] E. Nielsen, M. Akita, J. Davila-Aponte, and K. Keegstra. Stable association of chloroplastic precursors with protein translocation complexes that contain proteins from both envelope membranes and a stromal Hsp100 molecular chaperone. *EMBO J.*, 16:935–46, 1997.
- [72] M. Oreb, K. Reger, and E. Schleiff. Chloroplast protein import: reverse genetic approaches. *Curr. Genomics*, 7:235–44, 2006.
- [73] M. T. Paternostre, M. Roux, and J. L. Rigaud. Mechanisms of membrane protein insertion into liposomes during reconstitution procedures involving the use of detergents. 1. Solubilization of large unilamellar liposomes (prepared by reverse-phase evaporation) by triton X-100, octyl glucoside, and sodium cholate. *Biochemistry*, 27:2668–77, 1988.
- [74] R. Pecora. *Dynamic Light Scattering: Applications of Photon Correlation Spectroscopy*. Plenum, New York, 1985.
- [75] J. Pencer, G. F. White, and F. R. Hallett. Osmotically induced shape changes of large unilamellar vesicles measured by dynamic light scattering. *Biophys. J.*, 81:2716–28, 2001.
- [76] P. Pinnaduwege and B. D. Bruce. *In vitro* interaction between a chloroplast transit peptide and chloroplast outer envelope lipids is sequence-specific and lipid class-dependent. *J. Biol. Chem.*, 271:32907–15, 1996.
- [77] L. Plancon, M. Chami, and L. Letellier. Reconstitution of FhuA, an *Escherichia coli* outer membrane protein, into liposomes. Binding of phage T5 to Fhua triggers the transfer of DNA into the proteoliposomes. *J. Biol. Chem.*, 272:16868–72, 1997.
- [78] S. V. Provencher. A constrained regularization method for inverting data represented by linear algebraic or integral equations. *Comput. Phys. Comm.*, 27:213–27, 1982.

- [79] S. V. Provencher. Contin: a general purpose constrained regularization program for inverting noisy linear algebraic and integral equations. *Comput. Phys. Comm.*, 27:229–42, 1982.
- [80] M. Putman, H. W. van Veen, B. Poolman, and W. N. Konings. Restrictive use of detergents in the functional reconstitution of the secondary multidrug transporter LmrP. *Biochemistry*, 38:1002–8, 1999.
- [81] S. Qbadou, T. Becker, O. Mirus, I. Tews, J. Soll, and E. Schleiff. The molecular chaperone Hsp90 delivers precursor proteins to the chloroplast import receptor Toc64. *EMBO J.*, 25:1836–47, 2006.
- [82] A. Radunz. Localization of the tri- and digalactosyl diglyceride in the thylakoid membrane with serological methods. *Z. Naturforsch. [C]*, 31:589–93, 1976.
- [83] J. L. Rigaud. Membrane proteins: functional and structural studies using reconstituted proteoliposomes and 2-D crystals. *Braz. J. Med. Biol. Res.*, 35:753–66, 2002.
- [84] J. L. Rigaud and D. Levy. Reconstitution of membrane proteins into liposomes. *Methods Enzymol.*, 372:65–86, 2003.
- [85] J. L. Rigaud, G. Mosser, J. J. Lacapere, A. Olofsson, D. Levy, and J. L. Ranck. Bio-Beads: an efficient strategy for two-dimensional crystallization of membrane proteins. *J. Struct. Biol.*, 118:226–35, 1997.
- [86] G. Schatz. Just follow the acid chain. *Nature*, 388:121–2, 1997.
- [87] J. Scheuring, N. Braun, L. Nothdurft, M. Stumpf, A. K. Veenendaal, S. Kol, C. van der Does, A. J. Driessen, and S. Weinkauf. The oligomeric distribution of SecYEG is altered by SecA and translocation ligands. *J. Mol. Biol.*, 354:258–71, 2005.
- [88] E. Schleiff, M. Jelic, and J. Soll. A GTP-driven motor moves proteins across the outer envelope of chloroplasts. *Proc. Natl. Acad. Sci. USA*, 100:4604–9, 2003.
- [89] E. Schleiff and R. B. Klösgen. Without a little help from my friends: direct insertion of proteins into chloroplast membranes? *Biochim. Biophys. Acta*, 1541:22–3, 2001.
- [90] E. Schleiff, J. Soll, M. Küchler, W. Kühlbrandt, and R. Harrer. Characterization of the translocon of the outer envelope of chloroplasts. *J. Cell Biol.*, 160:541–51, 2003.
- [91] E. Schleiff, J. Soll, N. Sveshnikova, R. Tien, S. Wright, C. Dabney-Smith, C. Subramanian, and B. D. Bruce. Structural and guanosine triphosphate/diphosphate requirements for transit peptide recognition by the cytosolic domain of the chloroplast outer envelope receptor, Toc34. *Biochemistry*, 41:1934–46, 2002.
- [92] K. S. Schmitz. *An Introduction to Dynamic Light Scattering by Macromolecules*. Academic Press, New York, 1990.

- [93] D. J. Schnell, F. Kessler, and G. Blobel. Isolation of components of the chloroplast protein import machinery. *Science*, 266:1007–12, 1994.
- [94] S. M. Simon, C. S. Peskin, and G. F. Oster. What drives the translocation of proteins? *Proc. Natl. Acad. Sci. USA*, 89:3770–4, 1992.
- [95] C. Sirrenberg, M. F. Bauer, B. Guiard, W. Neupert, and M. Brunner. Import of carrier proteins into the mitochondrial inner membrane mediated by Tim22. *Nature*, 384:582–5, 1996.
- [96] M. D. Smith, C. M. Rounds, F. Wang, K. Chen, M. Afitlhile, and D. J. Schnell. atToc159 is a selective transit peptide receptor for the import of nucleus-encoded chloroplast proteins. *J. Cell Biol.*, 165:323–34, 2004.
- [97] K. Sohr and J. Soll. Toc64, a new component of the protein translocon of chloroplasts. *J. Cell Biol.*, 148:1213–21, 2000.
- [98] J. Soll, B. Bölter, R. Wagner, and S. C. Hinnah. ... response: the chloroplast outer envelope: a molecular sieve? *Trends Plant Sci.*, 5:137–8, 2000.
- [99] J. Soll and E. Schleiff. Protein import into chloroplasts. *Nat. Rev. Mol. Cell Biol.*, 5:198–208, 2004.
- [100] J. Soll and R. Tien. Protein translocation into and across the chloroplastic envelope membranes. *Plant Mol. Biol.*, 38:191–207, 1998.
- [101] Y. J. Sun, F. Forouhar, H. M. Li Hm, S. L. Tu, Y. H. Yeh, S. Kao, H. L. Shr, C. C. Chou, C. Chen, and C. D. Hsiao. Crystal structure of pea Toc34, a novel GTPase of the chloroplast protein translocon. *Nat. Struct. Biol.*, 9:95–100, 2002.
- [102] N. Sveshnikova, R. Grimm, J. Soll, and E. Schleiff. Topology studies of the chloroplast protein import channel Toc75. *Biol. Chem.*, 381:687–93, 2000.
- [103] N. Sveshnikova, J. Soll, and E. Schleiff. Toc34 is a preprotein receptor regulated by GTP and phosphorylation. *Proc. Natl. Acad. Sci. USA*, 97:4973–8, 2000.
- [104] Y. S. Teng, Y. S. Su, L. J. Chen, Y. J. Lee, I. Hwang, and H. M. Li. Tic21 is an essential translocon component for protein translocation across the chloroplast inner envelope membrane. *Plant Cell*, 18:2247–57, 2006.
- [105] P. W. van den Wijngaard and W. J. Vredenberg. The envelope anion channel involved in chloroplast protein import is associated with Tic110. *J. Biol. Chem.*, 274:25201–4, 1999.
- [106] C. van der Does, E. H. Manting, A. Kaufmann, M. Lutz, and A. J. Driessen. Interaction between SecA and SecYEG in micellar solution and formation of the membrane-inserted state. *Biochemistry*, 37:201–10, 1998.

- [107] C. van der Does, J. Swaving, W. van Klompenburg, and A. J. Driessen. Non-bilayer lipids stimulate the activity of the reconstituted bacterial protein translocase. *J. Biol. Chem.*, 275:2472–8, 2000.
- [108] A. Vasiljev, U. Ahting, F. E. Nargang, N. E. Go, S. J. Habib, C. Kozany, V. Panneels, I. Sinning, H. Prokisch, W. Neupert, S. Nussberger, and D. Rapaport. Reconstituted TOM core complex and Tim9/Tim10 complex of mitochondria are sufficient for translocation of the ADP/ATP carrier across membranes. *Mol. Biol. Cell*, 15:1445–58, 2004.
- [109] I. R. Vetter and A. Wittinghofer. The guanine nucleotide-binding switch in three dimensions. *Science*, 294:1299–304, 2001.
- [110] L. I. Viera, G. A. Senisterra, and E. A. Disalvo. Changes in the optical properties of liposome dispersions in relation to the interlamellar distance and solute interaction. *Chem. Phys. Lipids*, 81:45–54, 1996.
- [111] A. Villarejo, S. Buren, S. Larsson, A. Dejardin, M. Monne, C. Rudhe, J. Karlsson, S. Jansson, P. Lerouge, N. Rolland, G. von Heijne, M. Grebe, L. Bako, and G. Samuelsson. Evidence for a protein transported through the secretory pathway en route to the higher plant chloroplast. *Nat. Cell Biol.*, 7:1224–31, 2005.
- [112] A. Vojta, M. Alavi, T. Becker, F. Hörmann, M. Küchler, J. Soll, R. Thomson, and E. Schleiff. The protein translocon of the plastid envelopes. *J. Biol. Chem.*, 279:21401–5, 2004.
- [113] K. Waagemann and J. Soll. Characterization of the protein import apparatus in isolated outer envelopes of chloroplasts. *Plant J.*, 1:149–58, 1991.
- [114] K. Waagemann and J. Soll. Phosphorylation of the transit sequence of chloroplast precursor proteins. *J. Biol. Chem.*, 271:6545–54, 1996.
- [115] R. J. Wanders, W. F. Visser, C. W. van Roermund, S. Kemp, and H. R. Waterham. The peroxisomal ABC transporter family. *Pflugers Arch.*, in press, 2006.
- [116] P. H. Weigel, Z. Kyossev, and L. C. Torres. Phospholipid dependence and liposome reconstitution of purified hyaluronan synthase. *J. Biol. Chem.*, in press, 2006.
- [117] G. F. White, K. I. Racher, A. Lipski, F. R. Hallett, and J. M. Wood. Physical properties of liposomes and proteoliposomes prepared from *Escherichia coli* polar lipids. *Biochim. Biophys. Acta*, 1468:175–86, 2000.
- [118] J. C. Young, V. R. Agashe, K. Siegers, and F. U. Hartl. Pathways of chaperone-mediated protein folding in the cytosol. *Nat. Rev. Mol. Cell Biol.*, 5:781–91, 2004.

Acknowledgements

First of all, I want to thank my supervisor PD Dr. Enrico Schleiff for his guidance, discussion of ideas, constructive critique and support. I owe him special thanks for readiness to help in every situation and for nearly endless patience, which was often needed.

I would like to thank Prof. Dr. Jürgen Soll for the opportunity to do the research for my thesis as a member of his working group.

My thanks to Dr. Johannes Scheuring, Dr. Nikolaus Neumaier and Prof. Dr. Sevil Weinkauff for the collaboration on liposomes. I would also like to thank Dr. Ian Menz for the pMICO plasmid, and the group of Prof. Dr. Dirk Görlich for the Toc159 clone.

Many thanks to all my dear colleagues for helpful discussions and numerous little favors. Very special thanks to Thomas and Marko, who helped me a lot, especially in the beginning, and to Torsten, for interesting discussions and moral support. Thanks to Soumya, Mislav, Rolf, Tihana, Serena, Marcel, Lena, Johanna, Oli and Maike for interesting conversations and a nice working atmosphere.

Last, but not the least, my greatest thanks are reserved for my wife Lea, and for my parents. I would need a whole chapter to properly express my gratitude for their unconditional support.

Ehrenwörtliche Versicherung

Ich versichere hiermit ehrenwörtlich, dass die vorgelegte Dissertation von mir selbstständig und ohne unerlaubte Beihilfe angefertigt ist.

München, den 06. November 2006

Aleksandar Vojta

Erklärung

Hiermit erkläre ich, dass diese Dissertation keiner anderen Prüfungskommission weder in Teilen noch als Ganzes vorgelegt worden ist. Ich habe zuvor nicht versucht, anderweitig eine Dissertation einzureichen oder mich einer Doktorprüfung zu unterziehen.

München, den 06. November 2006

Aleksandar Vojta

Biography

Aleksandar Vojta

- 27.07.1979 Birth in Zagreb, Croatia
- 1985–1993 Elementary school in Zagreb
- 1993–1997 Classical Gymnasium in Zagreb
- 1997–2002 Study of Biology at the Faculty of Science, University of Zagreb
- 2002 Civil service
- since 11.2002 Doctoral study at the Botanical Institute, Faculty for Biology,
Ludwig-Maximilians-Universität Munich

Publications resulting from this work:

1. Vojta A, Scheuring J, Neumaier N, Mirus O, Weinkauff S, Schleiff E.
Determination of liposome size: a tool for protein reconstitution.
Anal. Biochem. (2005) **347**:24–33.
2. Clausen C, Ilkavets I, Thomson R, Philippart K, Vojta A, Mohlmann T,
Neuhaus E, Fulgosi H, Soll J.
Intracellular localization of VDAC proteins in plants.
Planta (2004) **220**:30–37.
3. Vojta A, Alavi M, Becker T, Hörmann F, Küchler M, Soll J, Thomson R, Schleiff E.
The protein translocon of the plastid envelopes.
J. Biol. Chem. (2004) **279**:21401–21405.
4. Becker T, Jelic M, Vojta A, Radunz A, Soll J, Schleiff E.
Preprotein recognition by the Toc complex.
EMBO J. (2004) **23**:520–530.

Lebenslauf

Aleksandar Vojta

- 27.07.1979 Geburt in Zagreb, Kroatien
- 1985–1993 Besuch der Grundschule in Zagreb
- 1993–1997 Besuch des Klassischen Gymnasiums in Zagreb
- 1997–2002 Studium der Biologie an der Wissenschaftlichen Fakultät, Universität Zagreb
- 2002 Zivildienst
- seit 11.2002 Promotion am Botanischen Institut, Fakultät für Biologie,
Ludwig-Maximilians-Universität München

Aus dieser Arbeit entstandene Publikationen:

1. Vojta A, Scheuring J, Neumaier N, Mirus O, Weinkauff S, Schleiff E.
Determination of liposome size: a tool for protein reconstitution.
Anal. Biochem. (2005) **347**:24–33.
2. Clausen C, Ilkavets I, Thomson R, Philippart K, Vojta A, Mohlmann T,
Neuhaus E, Fulgosi H, Soll J.
Intracellular localization of VDAC proteins in plants.
Planta (2004) **220**:30–37.
3. Vojta A, Alavi M, Becker T, Hörmann F, Küchler M, Soll J, Thomson R, Schleiff E.
The protein translocon of the plastid envelopes.
J. Biol. Chem. (2004) **279**:21401–21405.
4. Becker T, Jelic M, Vojta A, Radunz A, Soll J, Schleiff E.
Preprotein recognition by the Toc complex.
EMBO J. (2004) **23**:520–530.